Consequences of producing DNA gyrase from a synthetic *gyrBA* operon in *Salmonella enterica* serovar Typhimurium

German Pozdeev, Aalap Mogre and Charles J Dorman*

Department of Microbiology,
Moyne Institute of Preventive Medicine,
Trinity College Dublin
Dublin 2
Ireland

*For correspondence
cjdorman@tcd.ie

Corresponding author ORCID: https://orcid.org/0000-0002-6018-9170

Running title: *Salmonella* DNA gyrase operon

Summary

DNA gyrase is an essential type II topoisomerase that is composed of two subunits, GyrA and GyrB and has an A_2B_2 structure. Although the A and B subunits are required in equal proportions to form DNA gyrase, the *gyrA* and *gyrB* genes that encode them in *Salmonella* (and in many other bacteria) are at separate locations on the chromosome, are under separate transcriptional control, and are present in different copy numbers in rapidly growing bacteria. In wild-type *Salmonella*, *gyrA* is near the chromosome's replication terminus while *gyrB* is near the origin. We generated a synthetic *gyrBA* operon at the *oriC*-proximal location of *gyrB* to test the significance of the gyrase gene position for *Salmonella* physiology. Although the strain producing gyrase from an operon had a modest alteration to its DNA supercoiling set points, most housekeeping functions were unaffected. However, its SPI-2 virulence genes were expressed at a reduced level and its survival was reduced in macrophage. Our data reveal that the horizontally acquired SPI-2 genes have a greater sensitivity to disturbance of DNA topology than the core genome and we discuss its significance in the context Salmonella genome evolution and the *gyrA* and *gyrB* gene arrangements found in other bacteria.

Key words: *Salmonella enterica* serovar Typhimurium, DNA gyrase, *gyrA*, *gyrB*, DNA supercoiling, SPI-1, SPI-2

Introduction

DNA gyrase is an essential type II topoisomerase that introduces negative supercoils into DNA through an ATP-dependent mechanism (Gellert *et al*., 1976a; Higgins *et al.,* 1978; Nöllmann *et al*., 2007); it can also relax negatively supercoiled DNA via an ATP-independent mechanism (Gellert *et al*., 1977; Higgins *et al.,* 1978; Williams and Maxwell, 1999). The enzyme is composed of two copies of two subunits, GyrA and GyrB, giving it an A_2B_2 structure (Bates and Maxwell, 2005). Gyrase binds to DNA, makes a double-stranded cut, with 4-base overhangs, in the 'Gate' (or G) segment of the DNA and passes a nearby 'Transported' (or T) segment of intact DNA through the gap, changing the linking number of the DNA. The GyrA subunits form covalent bonds to the single-stranded DNA overhangs via tyrosine amino acids in their active sites while the GyrB subunits bind and hydrolyse ATP (Corbett and Berger, 2004).

Topoisomerase activity is required to eliminate the over-wound (positively supercoiled) and under-wound (negatively supercoiled) zones of the DNA template that are generated by transcription and DNA replication (Liu and Wang, 1987; Stracy et al., 2019). DNA gyrase relaxes the positively supercoiled DNA by introducing negative supercoils in an ATP-dependent manner (Ashley et al., 2017). Transcription and the associated disturbance to local DNA topology contribute to the architecture of the bacterial nucleoid by influencing the probability of DNA-DNA contacts between parts of the genome that border long transcription units that are heavily transcribed (Le and Laub, 2016). The changes to local DNA supercoiling that are caused by transcription and DNA replication also affect the activities of some transcription promoters (Ahmed et al., 2016; 2017; Chong et al., 2014; Dorman, 2019; Higgins, 2014; Rahmouni and Wells 1992; Rani and Nagaraja, 2019; Wu et al., 1988; Tobe et al., 1995).

The *in vivo* superhelical density of DNA in *Escherichia coli* is -0.025 (Bliska and Cozzarelli, 1987) and it has been estimated that the DNA of *E. coli* has 15% more supercoils than that of *Salmonella enterica* serovar Typhimurium (Champion and Higgins, 2007). Because a large subset of promoters is sensitive to alterations in DNA supercoiling and, to ensure

appropriate gene expression, topoisomerases are thought to play an important role in maintaining supercoiling set points within a range that is tolerable by the DNA transactions of the cell (Cheung et al., 2003; Dorman and Dorman, 2016; Peter et al., 2004; Sutormin et al., 2019). The promoters of *gyrA* and *gyrB*, the genes that encode the A and B subunits, respectively, of DNA gyrase, are stimulated by DNA relaxation (Menzel and Gellert, 1983; 1987; Straney et al., 1994; Unniraman and Nagaraja, 1999). This is part of a mechanism that maintains DNA supercoiling homeostasis, keeping average DNA supercoiling values within the tolerable range (DiNardo et al., 1982; Dorman et al, 1989; Pruss et al., 1982; Raji et al., 1985; Richardson et al., 1988; Steck et al., 1984). As a corollary to this, the transcription of *topA,* the gene encoding DNA topoisomerase I (Topo I), is stimulated by negative supercoiling (Ahmed et al., 2016; Tse-Dinh and Beran, 1988). Topo I relaxes negatively supercoiled DNA using an ATP-independent type I mechanism (Dekker *et al*., 2002).

Several studies have shown that gene position on the chromosome is physiologically significant in bacteria (Bogue et al., 2020; Bryant et al., 2014; Gerganova et al., 2015; Scholz et al., 2019). For example, moving the gene that encodes the nucleoid-associated protein FIS (Factor for Inversion Stimulation) from its native position, proximal to the origin of chromosome replication in *E. coli,* to locations close to the replication terminus, impaired the competitive growth fitness and altered the overarching network regulating DNA topology, resistance to environmental stress, hazardous substances and antibiotics (Gerganova et al., 2015). Among the genes that FIS regulates in *E. coli* (Schneider et al., 1999) and *S.* Typhimurium (Keane and Dorman, 2003) are *gyrA* and *gyrB*.

In *S.*Typhimurium, the *gyrA* and *gyrB* genes are widely separated on the genetic map of the circular chromosome: the *gyrB* gene is located close to the origin of chromosome replication, *oriC*, while *gyrA* is located near to the terminus region, Ter (McClelland et al., 2001). This arrangement closely resembles that seen in the model organism, *Escherichia coli* (Berlyn, 1998; Blattner et al., 1997). It has been proposed that the order of genes along each replichore in the bidirectionally replicated circular chromosome of *E. coli*

correlates with the peak levels of expression of genes as a culture passes through each of the major stages of its growth cycle in batch culture (Sobetzko et al., 2012). DNA supercoiling plays an important role in the initiation of chromosome replication, so locating *gyrB* close to *oriC* is consistent with the gene location hypothesis. Bacteria emerging from lag phase and entering a period of rapid growth in exponential phase, experience a build up of negative DNA supercoiling that stimulates the transcription of genes whose products support rapid growth (Colgan et al., 2018; Conter et al., 1997). Rapidly growing bacteria undergo multiple rounds of initiation of chromosome replication, so genes close to *oriC* are present in more copies per cell than those close to the terminus (Cooper and Helmstetter, 1968). GyrA and GyrB are required in equal amounts to form active DNA gyrase molecules, so the physical separation of *gyrA* from *gyrB* on the chromosome, and their organisation as independent transcription units, seem counterintuitive. In particular, why is *gyrA* so far away from *gyrB* on the circular chromosome of *S*. Typhimurium? The GyrA dimer is a stable structure that lends stability to the tetrameric DNA gyrase (Klostermeier, 2018). Perhaps placing *gyrA* close to the terminus of chromosome replication is well tolerated because a pool of GyrA is present in the cell throughout the growth cycle, available to interact with GyrB produced from the *gyrB* gene close to *oriC*. If this is so, why is this pattern not seen universally in bacteria? This may reflect species-specific differences gyrase subunit stabilities and in the ways that the GyrA and GyrB subunits interact in different bacteria (Weidlich and Klostermeier, 2020).

The genetically separated pattern of *gyrA* and *gyrB* gene location seen in *S*. Typhimurium and *E. coli* is not found universally among bacteria: many possess a *gyrBA* operon, although none appears to have a *gyrAB* operon. Perhaps this is unsurprising given that the functional domains in eukaryotic type II topoisomerases that are equivalent to the A and B subunits of DNA gyrase are always arranged in the order BA (Berger, 1998; Forterre et al., 2007) suggesting that the ancestor of eukaryotic type II topoisomerases was an operon with a *gyrBA* structure. Examples of other bacteria with a *gyrBA* setup include, *inter alia*, *Listeria monocytogenes* (Glaser et al., 2001),

Mycobacterium tuberculosis (Unniraman and Nagaraja, 1999; Unniraman et al., 2002) and *Staphylococcus aureus* (Baba et al., 2008). The operon arrangement appears to offer a number of advantages over the individual transcription unit model. Co-expression allows *gyrA* and *gyrB* to share the same promoter and the same transcription regulatory signals. Production of GyrA and GyrB from a common, bicistronic mRNA is likely to facilitate the establishment of equal amounts of each protein. The co-production of GyrA and GyrB might also be expected to enhance the efficiency of gyrase enzyme assembly. It should be noted that the *gyrA* and *gyrB* genes are only seen to be widely separated from one another on the unfolded, circular genetic map of *S*. Typhimurium: the genes may be brought into closer proximity in the folded chromosome within the nucleoid. Furthermore, in the tiny universe of the bacterium's interior, the problem of gyrase assembly from GyrA and GyrB subunits produced from spatially separated mRNA molecules may be an insignificant one (Moffitt et al., 2016). We investigated this issue by building a derivative of *S*. Typhimurium with a *gyrBA* operon and comparing its physiology with that of the wild type.

Results

Constructing a derivative of S*. Typhimurium with a synthetic* gyrBA *operon*

A kanamycin resistance cassette, *kan*, was inserted adjacent to the *gyrA* gene in *S*. Typhimurium strain SL1344 to serve as a selectable marker (Experimental procedures). This *gyrA-kan* combination was amplified by PCR, leaving behind the transcription control signals of *gyrA*, and inserted immediately downstream of the *gyrB* gene, creating a *gyrBA* operon with an adjacent *kan* gene that was bordered by directly-repeated copies of the FRT sequence; the *kan* gene was then deleted by FLP-mediated site-specific recombination at the *frt* sites. A *kan* gene cassette, flanked by directly repeated *frt* sites, was used to replace the *gyrA* gene at the native *gyrA* location in the *gyrBA*-operon-containing strain; this *kan* cassette was then excised by FLP-mediated recombination. This process produced a derivative of SL1344 that had a *gyrBA* operon at the chromosomal position that is normally occupied by only *gyrB* and had no *gyrA* gene at the chromosomal site where this gene normally resides (Fig. 1). The whole genome sequence of this new strain was determined to ensure that no genetic changes, other than the desired ones, were present; none was detected.

The growth characteristics of the gyrBA *operon strain*

The growth kinetics of the wild type and the strain with the *gyrBA* operon were compared in batch liquid culture. Cultures grown in Miller's lysogeny broth (LB) (Miller, 1972) had identical growth curves when measured by plating and colony counting or by optical density measurements (Fig. S1A, S1B). Growth was also assessed in a minimal medium in an experiment that included low magnesium stress, an important environmental challenge that *S*. Typhimurium encounters in the macrophage vacuole during infection (Colgan et al., 2018). The wild-type and the *gyrBA*-operon strains were grown in minimal medium N (Nelson and Kennedy, 1971) with either 10 μM (low magnesium) or 10 mM (high magnesium) $MgCl_2$. Once again, the two strains had identical growth kinetics (Fig. S1C).

Morphology of the strain with the gyrBA *operon*

The identical growth characteristics of the strain with the *gyrBA* operon and the wild type, both in LB and in minimal medium, showed that producing DNA gyrase from an operon made no difference to the growth cycle and suggested that the cell cycle was unlikely to be altered either. Interference with the timing of major events in the cell cycle (initiation, replication fork passage and termination) can lead to delays in cell division, resulting in filamentation of the bacterial cell (Martin et al., 2020; Sharma and Hill, 1995). When we compared the morphologies of mid-exponential-phase cultures of the wild type and the *gyrBA* operon strain by light microscopy, no differences in the shapes of the cells or the frequency of cell filamentation were detected (Fig. S2). Taken together with the growth kinetic data, these findings showed that the operonic arrangement of *gyrB* and *gyrA* is well tolerated by *S*. Typhimurium.

Sensitivity to gyrase-inhibiting antibiotics

The minimum inhibitory concentrations of gyrase-inhibiting antibiotics were compared for wild type SL1344 and SL1344 *gyrBA* (Fig. 2). Four drugs were tested: coumermycin and novobiocin are coumarins that target the GyrB subunit of DNA gyrase (Lewis et al., 1996) while nalidixic acid and ciprofloxacin are quinolones that target GyrA (Drlica and Zhao, 1997). Quinolones also target GyrB and coumarins and quinolones inhibit topoisomerase IV, the second type II topoisomerase found in *Salmonella* and related bacteria (Bush et al., 2020). The two strains were equally sensitive to the quinolones, but the SL1344 *gyrBA* strain was more resistant than SL1344 to novobiocin while SL1344 was more resistant than SL1344 *gyrBA* to coumermycin (Fig. 2). The reasons for the differential sensitivity patterns of the strains to the two classes of antibiotics, and for the opposing patterns of resistance to the two coumarins were not determined. Keeping in mind that the coumarins also target topoisomerase IV, we cannot be sure that the differences we observed do not reflect differences in the response of this second drug target in the SL1344 and SL1344 *gyrBA* strain. However, the results indicated that producing the subunits of gyrase from a *gyrBA* operon resulted in coumarin MIC data that were not equivalent to those measured for the strain producing the subunits from physically separate genes.

Motility and competitive fitness measurements

The *gyrBA* operon strain was compared with the wild type to assess relative motility on agar plates and competitive fitness in liquid co-culture. The operonic strain showed a small, but statistically significant, reduction in motility compared to the wild type (Fig. 3A). The reasons for this were not determined and may reflect changes at one or more levels in the production and operation of the complex motility machinery of the bacterium. In contrast, the two strains were equally competitive when growing in LB (Fig. 3B). To perform the competition, the two strains were each marked genetically by insertion on a chloramphenicol resistance (*cat*) cassette that is located in the pseudogene *SL1483*. This *cat* insertion has a neutral effect on fitness and serves simply to allow the competing bacteria to be distinguished by selection on chloramphenicol-containing agar (Lacharme-Lora et al., 2019). The competitions were performed between a *cat*-marked wild type and the unmarked *gyrBA* operon strain and separately between a *cat*-marked *gyrBA* operon strain and the unmarked wild type (Fig. 3B). No difference in the competitive indices of the two strains was detected in either version of the competition.

Transcription of the separate and the operonic gyr *genes*

The output of mRNA from the *gyrA* and *gyrB* genes was measured by quantitative PCR in wild type SL1344 and in SL1344 *gyrBA*, using the transcript of the *hemX* gene as a reference. (Expression of the *hemX* gene does not change under the growth conditions used here [Kröger *et al.*, 2013]). Gyrase gene transcription in both strains was found to vary with growth cycle stage, with mRNA outputs being highest in early exponential phase (2-h time point) and lowest in stationary phase (Fig. 4). In the wild type, the *gyrA* gene (located near Ter, the terminus of chromosome replication) was expressed to a significantly higher level than *gyrB* (located close to *oriC*) at 2 h. This was interpreted as a reflection of the need to compensate for the effect of increased *gyrB* gene dosage relative to that of *gyrA* in rapidly growing cells (Cooper and Helmstetter, 1968). As the culture approached stationary phase,

the levels of *gyrA* and *gyrB* transcripts equalised, in line with the convergence of *oriC*-proximal and Ter-proximal gene dosages (Fig. 4). The formation of the *gyrBA* operon eliminated the difference in *gyrB* and *gyrA* mRNA levels because each became part of the same bicistronic transcript and has adopted the expression profile of *gyrB* (Fig. 4).

DNA supercoiling in the strain with a gyrBA *operon*

The distributions of the topoisomers of the pUC18 reporter plasmid isolated from the wild type and the *gyrBA* operon strain were compared by electrophoresis in a chloroquine-agarose gel (Fig. 5). The cultures were grown in LB medium (Fig. 5A; S3A) or in minimal medium N with high or low concentrations of $MgCl_2$ (Fig. 5B; S3B). In LB, the reporter plasmid was more relaxed in the *gyrBA* strain than in the wild type (Fig. 5A, S3B). Low-magnesium growth was used to mimic one of the stresses experienced by *Salmonella* in the macrophage vacuole. In the high $MgCl_2$ control, the wild type and the *gyrBA* operon strain differed in their reporter plasmid distributions: DNA from the *gyrBA* strain was more negatively supercoiled than that from the wild type and showed a linking number difference (ΔLk) of -3 (Fig. 5b, S3B). At the low $MgCl_2$ concentration, the topoisomer distributions were more relaxed in both strains than in the high $MgCl_2$ controls (ΔLk = +3). The reporter plasmid from the *gyrBA* operon strain was also more negatively supercoiled than that from the wild type, with the peak in its topoisomer distribution being approximately 2 linking numbers below that of the wild type (Fig. 5B, S3B).

DNA relaxation occurs in *Salmonella* cells as they adjust to the macrophage vacuole; this forms part of the activation mechanism for the genes in the SPI-2 pathogenicity island (Cameron and Dorman, 2012; O Cróinín et al., 2006; Quinn et al., 2014). The products of these virulence genes protect the bacterium by inhibiting fusion of the vacuole with lysosomes (Garvis et al., 2001). We therefore monitored SPI-2 gene transcription in our two strains.

SPI-1 and SPI-2 gene expression in the gyrBA *operon strain*

290 The SPI-1 and SPI-2 pathogenicity islands encode distinct type 3 secretion
291 systems and effector proteins that are used to invade epithelial cells (SPI-1)
292 or to survive in the intracellular vacuole (SPI-2) (Figueira and Holden, 2012;
293 Hensel, 2000; van der Heijden and Finlay, 2012). Transcription of SPI-1
294 genes was monitored using a *gfp*$^+$ reporter fusion under the control of the
295 *prgH* promoter, $P_{prgH,}$ while a *gfp*$^+$ fusion to the *ssaG* promoter (P_{ssaG}) was
296 used to monitor SPI-2 gene transcription. Wild type and *gyrBA* operon strains
297 harbouring these fusions were grown in LB medium (Fig. 6A, 6B) or in
298 minimal medium N, supplemented with high or low concentrations of $MgCl_2$.
299 (Fig. 6C-F). The cultures were grown with aeration at 37˚C in 96-well plates,
300 and green fluorescence was measured throughout the growth cycle. The
301 results obtained showed that in LB medium and in minimal medium N, SPI-1
302 transcription was indistinguishable between the wild type and the *gyrBA*
303 operon strains (Fig. 6A, 6C, 6E). SPI-2 transcription was equivalent in both
304 strains growing in LB (Fig. 6B) or in minimal medium with high $MgCl_2$ (Fig.
305 6D). However, SPI-2 transcription occurred at reduced levels in the *gyrBA*
306 strain in the later stages of the growth cycle under low magnesium conditions
307 (7.8% lower between the 800- and 1460-minute time points in Fig. 6F). These
308 findings showed that when the subunits of gyrase are produced from an
309 operon, rather than from separate *gyrA* and *gyrB* genes in their native
310 chromosome locations, the normal expression profile of the SPI-2 virulence
311 gene cluster is disrupted, but that this is conditional on growth in a low
312 magnesium medium.
313
314 *Impact of the gyrase operon on cell infection by* Salmonella
315 The abilities of the wild type and the *gyrBA* operon strains to invade and to
316 replicate in cultured mammalian cells were compared. Bacteria, grown to mid-
317 exponential phase to promote SPI-1 gene expression, were used to infect
318 RAW264.7 macrophage. When intracellular bacteria were then enumerated
319 post-invasion, fewer of the *gyrBA* operon strain cells were detected than wild
320 type cells at and after the 16-h time point (Fig.7). This reduction in bacterial
321 survival correlated with the diminished SPI-2 expression detected in the
322 *gyrBA* operon strain in low Mg^{2+}, a macrophage relevant condition.

Discussion

The genes in *Salmonella* that encode DNA gyrase, *gyrA* and *gyrB*, are located at the opposite ends of the left replichore of the chromosome (Fig. 1). In contrast, many other bacteria, such as *Listeria monocytogenes, Staphylococcus aureus* and *Mycobacterium tuberculosis*, possess a *gyrBA* operon (Baba et al., 2008; Glaser et al., 2001; Unniraman and Nagaraja, 1999; Unniraman et al., 2002). As a first step in assessing the significance of the stand-alone gyrase gene arrangement versus the operon model, we constructed a derivative of *S*. Typhimurium with a *gyrBA* operon at the chromosomal location that is normally occupied by *gyrB* alone, while removing the individual *gyrA* gene from its native position in the genome. This strain, with the *gyrB* and *gyrA* genes transcribed from a common promoter (P_{gyrB}) and located close to the origin of chromosomal replication, had normal growth characteristics (Fig. S1) and cell morphology (Fig. S2).

Although the production of DNA gyrase from an operon was well tolerated by *S.* Typhimurium, the operon strain differed from the wild type in a number of phenotypic characteristics. These included a modest decrease in competitive fitness in the operon strain (Fig. 3) that hinted at generalised impacts on physiology. There were subtle differences in sensitivities to coumarin antibiotics, but not quinolones, that distinguished the operon strain from the wild type (Fig. 2). In *E. coli*, the *gyrA* and *gyrB* genes respond differently to treatment with DNA gyrase inhibitors: while coumarins and quinolones both increase the expression of *gyrA*, the expression of only *gyrB* is induced by coumarins (Neumann & Quiñones, 1997). In our operon strain, the coumarin-sensitive *gyrB* promoter drives the transcription of both *gyrB* and *gyrA,* and this may have contributed to the difference between the operon strain and the wild type in responding to coumarin challenge. It is also possible that the differences in coumarin sensitivity may have involved indirect effects of operonic gyrase production on processes involved in drug uptake and/or be due to differential effects on the activity of the bacterium's second coumarin target, topoisomerase IV, in the wild type and gyrase operon strains.

The stand-alone *gyrA* gene is expressed to a higher level than *gyrB* in the wild type, albeit from a distant location on the chromosome (Fig. 4). Also,

the stable GyrA protein seems to play a foundational role in the assembly of DNA gyrase (Klostermeier, 2018; Weidlich and Klostermeier, 2020). Placing the *gyrA* gene under the control of the P_{gyrB} promoter in the *gyrBA* operon equalised the levels of the transcripts from the two genes (Fig. 4) by making them parts of a bicistronic operon (Fig. 1). Operon formation, with the associated equalising of *gyrB* and *gyrA* transcript levels, may have altered the cellular ratio of GyrB and GyrA, as well as their site of production, in ways that produced the effects we have detected on DNA topology, coumarin sensitivity, SPI-2 expression and *Salmonella* virulence.

The expression of the horizontally acquired SPI-2 pathogenicity island allows *S.* Typhimurium, a facultative intracellular pathogen, to survive in the hostile environment of the macrophage vacuole. The *gyrBA* operon strain both expressed SPI-2 less well (Fig. 6) and survived less well than the wild type in the macrophage (Fig. 7). The *Salmonella*-containing vacuole of the macrophage is a stressful, low magnesium environment where the SPI-2-encoded type 3 secretion system and its associated effector proteins, play a key protective role (Figueira and Holden, 2012; Hensel, 2000; van der Heijden and Finlay, 2012). DNA relaxation contributes to full expression of SPI-2 genes (Cameron and Dorman, 2012; Quinn et al., 2014) and DNA in *S.* Typhimurium becomes relaxed when the bacterium is in the macrophage (O Cróinín et al., 2006), The *gyrBA* operon strain maintained its DNA in a less relaxed state in a low-magnesium environment (Fig. 5) and this may explain the poorer transcription of SPI-2 that was seen in low magnesium growth (Fig. 6).

Our data reveal a distinction between the sensitivity of genes encoding housekeeping functions and genes in the horizontally acquired accessory genome to the production of DNA gyrase from an operon. Genes that have been acquired by *Salmonella* via horizontal gene transfer (HGT) are more A+T-rich than core genome members and are subject to multifactorial control that includes a prominent role for nucleoid-associated proteins such as H-NS, FIS, IHF and HU (Banda et al., 2019; Cameron and Dorman, 2012; Dillon and Dorman, 2010; Fass and Groisman, 2009; Mangan et al., 2006; 2011; Quinn et al. 2014). These genes also display sensitivity to changes in DNA topology

(Cameron and Dorman, 2012; O Cróinín et al., 2006; Quinn et al., 2014). SPI-2 expression is held in check in *Salmonella* until it is required during adaptation to the macrophage vacuole and a shift in global DNA supercoiling levels is a component of the activation signal (Cameron and Dorman, 2012; O Cróinín et al., 2006; Quinn et al., 2014). The shift in global DNA supercoiling values that we see in *Salmonella,* growing in a minimal medium that mimics the intravacuolar environment, dysregulates SPI-2 transcription and compromises *Salmonella* infectivity. This finding is consistent with proposals that *Salmonella* maintains a level of DNA topology that is optimised to control the activities, and the expression, of mobile genetic elements that include pathogenicity islands, bacteriophage and transposons (Cameron et al., 2011; Champion and Higgins, 2007; Higgins, 2016).

We have shown experimentally that there is no absolute barrier to the organisation of the *gyrB* and *gyrA* genes as a *gyrBA* operon in *Salmonella*. Furthermore, there are many examples of naturally occurring *gyrBA* operons among bacterial species. Why is this arrangement not found universally? Sharing a common promoter, common transcriptional regulatory features and a common chromosomal location would appear to offer the advantages of coordinated gene expression (Price et al., 2005) and physical co-production of protein products that will need to combine with a fixed stoichiometry to form an active product (Dandekar et al., 1998; Pal and Hurst, 2004; Swain, 2004). Indeed, the coupling of transcription and translation in prokaryotes may aid the production of operon-encoded proteins that are required in stoichiometric amounts (Li et al., 2014; Rocha, 2008). Often, but not invariably, operons are composed of genes that contribute to a common pathway (de Daruvar et al., 2002; Lawrence and Roth, 1996; Price et al., 2006; Rogozin et al., 2002) and that is true of the *gyrBA* operon. Colocation of genes within an operon facilitates their collective translocation via horizontal gene transfer, allowing them to replace lost or mutated copies in the recipient cell (Lawrence and Roth, 1996). According to this "selfish operon" hypothesis, this creates a selective pressure for the maintenance of an operon structure. However, since loss of either *gyrA* or *gyrB* is lethal, the gyrase operon may be one of

421 the exceptions to the selfish operon rule, because gyrase-deficient recipients
422 cannot exist.
423 We conducted a survey of gyrase gene locations in bacteria to assess
424 the frequency of the stand-alone arrangement seen in *Salmonella* and the
425 *gyrBA* operon arrangement seen in other species (Experimental procedures).
426 We were unable to find any example of a bacterium with a *gyrAB* operon. It
427 should be noted that the functional domains corresponding to GyrA and GyrB
428 in eukaryotic type II topoisomerases are found in the order BA (Berger, 1998;
429 Forterre et al., 2007), suggesting that their ancestor may have been encoded
430 by an operon with a *gyrBA* structure. The results of the survey are shown in
431 Table 1, where bacteria are grouped according to their gyrase gene
432 arrangement, using *oriC* as a reference point. Fig. 8 shows a phylogenetic
433 tree summarising the occurrence of different gyrase gene arrangements
434 among bacteria from the four groups listed in Table 1.
435 Inversions of DNA between the left and the right replichores were seen
436 frequently and these followed no obvious patterns. This is in agreement with a
437 previous finding that, while distance to the origin is highly conserved,
438 inversions of genes around the Ter region of a chromosome are frequent and
439 well tolerated in *E. coli* and *Salmonella* (Alokam *et al.*, 2002). Various relative
440 arrangements of *gyrA* and *gyrB* were observed and subdivided into four
441 groups: Group 1 had *gyrB* and *gyrA* positioned separately, with *gyrB* near
442 *oriC*; Group 2 had *gyrB* and *gyrA* positioned separately, with the position of
443 *gyrB* being variable; Group 3 had *gyrB* and *gyrA* arranged as a *gyrBA* operon
444 in the immediate vicinity of *oriC*; Group 4 had *gyrB* and *gyrA* arranged as a
445 *gyrBA* operon at a distance from *oriC*. The arrangements of *gyrA* and *gyrB*
446 genes were categorised into the four Groups not only according to the relative
447 positions of *gyrA* and *gyrB,* but also according to the degree of conservation
448 of the genetic environment of *gyrB*.
449 Table 1 suggests that all members of the class gamma-proteobacteria
450 (phylum Proteobacteria), including *E. coli* and *Salmonella*, some alpha-
451 proteobacteria, beta-proteobacteria and epsilon-proteobacteria are in Group
452 1. Group 2 contains some alpha-, beta- and delta-proteobacteria, members of
453 the family *Streptococcaceae* (order Lactobacillales, phylum Firmicutes);

454 members of the class Flavobacteriia; multiple members of the phylum
455 Bacteroidetes; Acidobacteria and *Deinococcus radiodurans*. Group 3 was
456 composed of members of the phylum Actinobacteria, classes Clostridia and
457 Bacilli (phylum Firmicutes), family *Enterococcaceae* and family
458 *Lactobacillaceae* (order Lactobacillales, phylum Firmicutes) order
459 Fusobacteria (phylum Fusobacteria) and phylum Terenicutes. Finally, Group 4
460 consisted of members of the phylum Chlamydiae. There is perhaps more
461 variation within Group 4, but this was not detected using the method
462 employed here. *Mycoplasma* is an anomaly of Group 3, since not all its
463 species clearly belong to this group. Some *Mycoplasma* possess the
464 expected conserved genes 5' to *gyrB,* but not in its immediate vicinity.
465 However, the orientation of genes 5' to *gyrB* remains favourable for the
466 initiation of its transcription, therefore, *Mycoplasma* is placed in Group 3. It
467 was clear from the analysis that members of the same taxonomic rank do not
468 necessarily have to belong to the same Group, especially in diverse phyla.
469 For example, both Group 2 and Group 3 arrangements are present within the
470 Firmicutes. Moreover, both arrangements are present within the order
471 Lactobacillales alone. Some less diverse phyla such as Fusobacteria and
472 Chlamydiae belong to only one Group. No variation was found within families.
473 It was difficult to conclude if given taxons were enriched in particular
474 groups in Table 1, so a phylogenetic tree was plotted that included all of the
475 bacteria in the table (Fig. 8). The tree was constructed using the phylogenetic
476 tree generator phyloT, based on NCBI taxonomy (Letunic & Bork, 2019) and
477 the positions of the branches were manually reviewed with the aid of the NCBI
478 taxonomy browser. It is apparent that one Group can be present in multiple
479 unrelated phyla and that one phylum can contain members of several Groups,
480 illustrating a high level of diversity of *gyrA* and *gyrB* chromosomal
481 arrangements. However, certain patterns are discernable. Bacteria from
482 Group 1 are exclusively located in phylum Proteobacteria. All the members of
483 phylum Bacteroidetes that were investigated belong to Group 2, but other
484 phyla can also contain some members of Group 2. The Group 3 arrangement
485 occurs with high frequency in the superphylum Terrabacteria (Firmicutes,
486 Tenericutes, Actinobacteria, Deinococcus), although this arrangement can be

encountered elsewhere too. Finally, all of the tree members of Group 4 shown belong to the phylum Chlamydiae. No other phylum was found to contain bacteria of Group 4, but the existence of the Group 4 arrangement outside of the Chlamydiae cannot be ruled out. It is also difficult to draw clear parallels between the lifestyle of an organism and the Group to which it belongs, since bacteria of various lifestyles can be members of the same Group. The analysis presented here is indicative rather than exhaustive: it is possible that further sampling will broaden the existing Groups and reveal further details.

When the immediate genetic environment of both genes in bacteria listed in Table 1 was studied, one distinct pattern was found – homologues of *dnaA* (encoding chromosomal replication initiation protein DnaA), *dnaN* (encoding the beta subunit of DNA polymerase III) and *recF* (encoding the DNA repair protein RecF) or at least one of these three genes, are found directly upstream of *gyrB* gene in all bacteria in which *gyrB* is located in the immediate vicinity of *oriC*, such as most bacteria of Groups 1 and 3 (Table 1). Transcription from these co-oriented neighbouring genes provides a strong input of DNA relaxation (Sobetzko, 2016) that stimulates transcription of the supercoiling-sensitive *gyrB* promoter, P_{gyrB} (Menzel & Gellert, 1987). This is true of most bacteria where *gyrB* is in the immediate vicinity of *oriC* and *gyrA* is located either about 20% of the chromosome further away or is a part of a *gyrBA* operon. Bacteria with a *gyrBA* operon that is not in the immediate vicinity of *oriC* (such as *Chlamydia psittaci*) and bacteria with the two *gyr* genes separated by about 20% of the chromosome, such as *Myxococcus xanthus* (together with some Bacteroidetes) that satisfy the gene positional parameters characteristic of Group 1, possess *gyrB* with a non-conserved genetic neighbourhood. Bacteria of Groups 2 and 4 do not have a conserved genetic environment around *gyrB*. The conservation of the genetic neighbourhood 5' to *gyrB* seems to be more important than the subjective proximity to *oriC*. Therefore, genetic neighbourhood conservation was used as a parameter to decide the groupings in Table 1. The frequent association of *gyrB* with the *dnaA*, *dnaN* and *recF* genes; the higher conservation of *gyrB*'s position in comparison to *gyrA*; the transcriptional response of *gyrB* to quinolones– all indicate that conservation of the physical location of *gyrB,* but

not *gyrA,* is essential in many bacteria. These findings reveal important information about chromosome composition in natural bacteria and can help guide attempts at synthetic chromosome design.

Experimental procedures

Bacterial strains and culture conditions

The bacterial strains used in this study were derivatives of *S.* Typhimurium strain SL1344 and their details are listed in Table 1. Bacterial cultures were grown routinely either in Miller's lysogeny broth (LB) (Miller, 1972) or in minimal medium N (Nelson and Kennedy, 1971). Bacteriophage P22 HT 105/1 *int*-201 was used for generalized transduction during strain construction (Schmieger, 1972). Phage lysates were filter-sterilized and stored at 4°C in the dark. Bacterial strains were stored as 35% glycerol stocks at -80°C and freshly streaked on agar plates for each biological replicate. Four ml LB broth was inoculated with a single colony and grown for 18 h. This overnight culture was sub-cultured into fresh 25 ml LB broth normalizing to an OD_{600} of 0.003, unless otherwise stated, and grown to the required growth phase. The standard growth conditions for all bacterial strains were 37°C, 200 rpm, unless otherwise stated. For culturing in minimal medium, overnight cultures were prepared as described above. 1 ml of overnight culture was washed three times with minimal medium N of the required $MgCl_2$ concentration to remove nutrients, sub-cultured into minimal medium of the corresponding $MgCl_2$ concentration in a total volume of 25 ml and grown for 24 h to pre-condition the bacteria. The pre-conditioned culture was sub-cultured into 25 ml of fresh minimal medium N adjusted to an OD_{600} of 0.03 and grown for a further 24 h to obtain a culture in the stationary phase of growth.

To measure growth characteristics of a bacterial culture, an overnight culture was adjusted to an OD_{600} of 0.003 in 25 ml of fresh LB broth and grown at the standard conditions for 24 h in the appropriate liquid medium. The optical density of the culture at OD_{600} was measured at 1-h intervals for the first 3 hours and then every 30 min until 8 hours; the last reading was taken at 24 h. Measurements were taken using a Thermo Scientific BioMate 3S spectrophotometer with liquid cultures in plastic cuvettes. To measure the growth characteristics of a bacterial culture in minimal medium with altered Mg^{2+} concentration, an overnight bacterial culture was washed in minimal medium with an appropriate concentration of

$MgCl_2$ and pre-conditioned for 24 h. The pre-conditioned culture was adjusted to an OD_{600} of 0.03 in 25 ml of fresh medium in two flasks and the OD_{600} was measured every hour beginning from 2 h post time zero until 8 h. Separate cultures were set up similarly to measure OD_{600} every hour from 8 h until 15 h. In this way, the number of times each flask was opened and sampled was minimized to yield reliable and reproducible measurements.

The growth characteristics of bacterial cultures in LB broth were also measured by viable counts. The culture was grown in the same way as for spectrophotometry, and an aliquot was taken at 2 h, 4 h, 6 h, 8 h and 24 h, serially diluted and spread on LB agar plates to give between 30 and 300 colonies after overnight incubation at 37°C. The bacterial colony counts were expressed as colony forming units per millilitre (cfu ml^{-1}).

Bacterial motility assays

Assays were carried out precisely as described to achieve agreement between biological replicates. 0.3% LB agar was melted in a 100 ml bottle in a Tyndall steamer for 50 min, allowed to cool in a 55°C water bath for 20 min, six plates were poured and left to dry near a Bunsen flame for 25 min. 1 µl of bacterial overnight culture was pipetted under the agar surface with two inocula per plate. Plates were placed in a 37°C incubator without stacking to ensure equal oxygen access. After 5 h, the diameters of the resulting swarm zones were measured and expressed as the ratio of the WT zone to that of the mutant.

Competitive fitness assays

Flasks of broth were inoculated with the pair of competing bacterial strains in a 1:1 ratio. Derivatives of each competitor were constructed that carried a chloramphenicol acetyl transferase (*cat*) gene cassette within the transcriptionally silent pseudogene *SL1483*. This *cat* insertion is known to be neutral in its effects on bacterial fitness (Lacharme-Lora et al., 2019) and allows the marked strain to be distinguished from its unmarked competitor. Competitions were run in which wild type SL1344 was the marked strain or in which SL1344 *gyrBA* was the marked strain. Strains to be competed were

pre-conditioned in separate 25 ml cultures for 24 h without antibiotics. Then 10^5 cells of each strain were mixed in 25 ml of fresh LB broth and grown as a mixed culture for another 24 h. The number of colony forming units was determined by plating the mixture on chloramphenicol-containing plates and on plates with no antibiotic at T=0 h and T=24 h. Taking the wild type SL1344 Vs SL1344 *gyrBA* competition as an example, SL1344 was competed against SL1344 *gyrBA SL1483::cat* and, as a control, SL1344_*SL1483::cat* was competed against SL1344 *gyrBA*. The competitive fitness index (f.i.) was calculated according to the formula:

$$\text{f.i.} = (\ln (Nc(24)/Nc(0)))/(\ln ((Nwt(24)/Nwt(0)))),$$

where Nc(0) and Nc(24) are the initial and final counts of a competitor and Nwt(0) and Nwt(24) are initial and final counts of the WT. Competitor is a strain other than the WT; f.i. <1 means that the competitor is less fit than the WT; f.i.>1 indicates the opposite.

Construction of a gyrBA *operon strain*

A derivative of *S.* Typhimurium with an artificial *gyrBA* operon was constructed by Lambda-Red homologous recombination (Datsenko & Wanner, 2000). Briefly, a *kan* cassette was amplified from plasmid pKD4 with primers Kan ins gyrA F and Kan ins gyrA R, (Table S1) using Phusion high-fidelity DNA polymerase. The amplicon, with overhangs homologous to a region immediately downstream of *gyrA,* was transformed into the WT strain harbouring plasmid pKD46, then grown in the presence of arabinose to activate the Lambda Red system in order to tag *gyrA* with the *kan* cassette. The *gyrA*::*kan* construct, including 20 nucleotides upstream from the *gyrA* translational start codon, was amplified using primers gyrB.int.gyrA::kan_Pf and gyrB.int.gyrA::kan_Prev (Table S1). The amplicon had overhangs that were homologous to sequences immediately downstream of *gyrB.* This allowed translation of the GyrA protein from the bicistronic *gyrBA* mRNA because several sequences closely matching to a consensus ribosome binding site (5'-AGGAGG-3') were located in this 20 bp region. The *gyrA*::*kan* amplicon was inserted by Lambda Red-mediated recombination immediately downstream of the *gyrB* protein-coding region to construct the *gyrBA* operon.

622 The original *gyrA* gene was deleted by an in-frame insertion of a *kan* cassette
623 (Baba *et al.*, 2006). The *kan* resistance cassettes were subsequently
624 eliminated via FLP-mediated site-specific recombination (Cherepanov &
625 Wackernagel, 1995). The resulting *gyrBA* strain had the genes that encode
626 both subunits of DNA gyrase arranged as a bicistronic operon under the
627 control of a common promoter, P_{gyrB} (Table 2).
628
629 *DNA isolation for whole genome sequencing*
630 To obtain high-quality chromosomal DNA for whole genome sequencing, a
631 basic phenol-chloroform method was used (Sambrook & Russell, 2006). 2 ml
632 of an overnight culture were centrifuged at 16000 x g for 1 min to harvest cells
633 and the cell pellet was resuspended in 400 µl of TE buffer pH 8 (100 mM Tris-
634 HCl pH 8.0, 10 mM EDTA pH 8.0 (BDH, Poole, England)). 1% SDS and 2
635 mg/ml proteinase K were added and incubated for 2 h at 37°C to complete
636 lysis. DNA was isolated by the addition of 1 volume of phenol pH 8.0 :
637 chloroform : isoamyl alcohol (25 : 24 : 1) (AppliChem, Darmstadt, Germany),
638 thorough mixing and centrifugation at 16000 x g for 15 min at 4°C in phase-
639 lock tube. The upper aqueous layer containing DNA was collected and the
640 phenol: chloroform extraction was repeated two more times. To remove
641 contaminants and to precipitate DNA, sodium acetate pH 5.2 at 0.3 M and
642 isopropanol at 60% of the final volume were added and kept for 1 h at -20°C.
643 DNA was pelleted by centrifugation at 16000 x g for 15 min at 4°C. The DNA
644 pellet was washed with 70% ethanol, dried at 37°C until translucent and
645 resuspended in 100 µl TE pH 8.0. The sample was electrophoresed on
646 agarose gel to check for degradation and the DNA concentration was
647 determined as follows: to remove RNA contamination from DNA samples, 100
648 mg/ml RNase A was added and incubated for 30 min at 37°C. Phenol-
649 chloroform extraction was performed as above. To precipitate DNA, 0.5 M of
650 ammonium acetate (Merck, Darmstadt, Germany) and a half volume of
651 isopropanol were added and incubated for 2 h at -20°C. DNA was pelleted by
652 centrifugation at 16000 x g for 15 min at 4°C. The DNA pellet was washed
653 twice with 70% ethanol, dried at 37°C until translucent and resuspended in 50
654 µl water. The sample was run on an agarose gel to check for degradation.

The concentration of DNA extracted was determined by measuring absorbance at 260 nm on a DeNovix DS-11 spectrophotometer (Wilmington, Delaware, USA). The shape of the absorbance curve was ensured to have a clear peak at 260 nm. The purity of samples was assessed by the ratio of A_{260}/A_{280} – a measure of protein and phenol contamination and A_{260}/A_{230} – a measure of contaminants such as EDTA, where both should be as close as possible to 2. Only high-quality samples were chosen for further work.

Whole genome sequencing

Whole genome sequencing was performed on final versions of the constructed strains to ensure that no compensatory mutations were introduced into their genomes. The sequencing was performed by MicrobesNG (Birmingham, UK) using Illumina next generation sequencing technology. The output reads were assembled using Velvet (Zerbino, 2010) and aligned to the reference SL1344 sequence NC_016810.1 Breseq software (Deatherage & Barrick, 2014). The data are available through the Sequence Read Archive (SRA) with accession number PRJNA682874.

RNA extraction, DNase treatment and RT-qPCR.

RNA for measuring gene expression by qPCR was isolated using an acidic phenol-chloroform method. An overnight culture was subcultured into 25 ml of fresh LB broth normalising to an OD600 of 0.003. The bacterial culture was grown to the required timepoint and mixed with 40% volume of 5% acidic phenol (pH 4.3) in ethanol and placed on ice for at least 30 min to stop transcription. The cells were harvested by centrifugation at 3220 x g for 10 min at 4°C and resuspended in 700 µl of TE buffer pH 8 containing 0.5 mg/ml lysozyme. 1% SDS and 0.1 mg/ml proteinase K were added and incubated for 20 min at 40°C to complete lysis. 1/10 volume of 3 M sodium acetate was added to precipitate RNA, 1 volume of 1:1 solution of acidic phenol and chloroform was added, mixed well on a vortex mixer and centrifuged at 16000 x g for 15 min at 4°C to extract RNA into aqueous phase. To precipitate RNA the aqueous layer was harvested, mixed with 1 volume of isopropanol and incubated at -20°C for 1 hour. RNA was harvested by centrifugation at 16000

x g for 15 min at 4°C. The RNA pellet was washed with 70% ethanol and dried at 37°C until translucent. The total RNA was dissolved in 50 µl DEPC-treated water and its concentration was determined using DeNovix DS-11 spectrophotometer.

For DNase-treatment, RNA was diluted to 20 µg in 80 µl, denatured at 65°C for 5 min and kept on ice. 1x DNase I buffer including MgCl2 and 10 U DNase I (ThermoFisher Scientific, Waltham, US) were added and incubated for 45 min at 37°C. 100 µl of 1:1 acidic phenol : chloroform was added to DNase I digestion samples, mixed and transferred to a phase-lock tube. RNA was extracted by centrifugation at 16000 x g for 12 min at 15°C. The upper aqueous layer was harvested and RNA was precipitated by adding 2.5 volumes of 30:1 ethanol : 3 M sodium acetate pH 6.5 for 2 h or overnight at -20°C. RNA was harvested by centrifugation at 16000 x g for 30 min at 4°C. The RNA pellet was washed with 70% ethanol and dried at 37°C until translucent. The total RNA was dissolved in 30 µl DEPC-treated water and its concentration was determined as in 2.5.5. RNA was checked for DNA contamination by the end point PCR and for integrity on a HT gel (Mansour & Pestov, 2013).

400 nm of the total extracted and DNase I treated RNA was converted to cDNA using GoScriptTM Reverse Transcription System kit (Promega) according to manufacturer's guidelines. Then, 5.33 ng of cDNA in 20 µl reaction was used as a template for Real Time quantitative PCR (RT-qPCR) using 1x FastStart Universal SYBR Green Master (ROX) (Roche, Mannheim, Germany) and gene-specific pair of primers (0.3 µM each). For each pair of primers, a standard curve was generated using 10-fold serially diluted gDNA. PCR and fluorescence detection were carried out in StepOne Real Time PCR system (Applied Biosystems). Analysis was performed in the accompanying software. The cycling conditions were as follows:
10 min at 95°C; 40 cycles of 15 sec at 95°C and 1 min at 60°C.

Minimum inhibitory concentration (MIC) of antibiotics determination

MIC90 of antibiotics (a minimal concentration at which 90% of bacterial growth is inhibited) was found by serially diluting antibiotics and

spectrophotometrically testing the ability of different dilutions to inhibit bacterial growth. On a 96-well plate, all wells (excluding column 12) were filled with 60 µl of sterile LB broth. 1 ml solutions of antibiotics to be tested were prepared at the highest desired concentration in LB. 300 µl of the prepared antibiotics were added to the wells of column 12 and homogenised by pipetting up and down 5 times with a multichannel pipette. 240 µl was transferred to the next wells in column 11, homogenisation was repeated and serial 1:1.25 dilutions were sequentially continued until column 3. The final 240 µl from column 3 were discarded. All the wells were inoculated with bacterial cultures adjusted to an OD_{600} of 0.003 except column 1. In this way column 1 contained negative controls (no bacteria and no antibiotic), column 2 contained positive controls (no antibiotics) and columns 3-12 contained serially diluted antibiotics inoculated with the identical number of bacteria. The plate was covered, sealed between plastic sheets and incubated for 18 h at the standard growth conditions. The plate was read by measuring OD_{600} values on a plate reader (Multiscan EX, Thermo Electronics).

SPI-1 and SPI-2 reporter assays

Salmonella pathogenicity island (SPI) activity was accessed by measuring the expression of *gfp*$^+$ reporter gene fusions to promoters of *prgH* and *ssaG* to look at SPI-1 and SPI-2 expression, respectively. The *gfp*$^+$ reporter fusions were transduced into each strain by P22 generalized transduction and selected with chloramphenicol. 100 µl of overnight culture of the *gfp*$^+$ reporter-carrying strain was diluted 1:100 in LB broth. Black 96 plate with transparent flat bottom was filled with 100 µl of the diluted culture in six technical replicates, negative controls were included. The plate was sealed with parafilm and incubated at 300 rpm, 37°C for 24 h in the Synergy H1 microplate reader (Biotek, Vermont, USA). Bacterial growth was measured at 600 nm and GFP fluorescence was read using 485.5 nm excitation frequency at 528 nm emission frequency, measurements were taken every 20 min. For measurements in the minimal medium, the culture was adjusted to OD_{600} of 0.03 in the medium of the required $MgCl_2$ concentration and measurements proceeded as above.

Global supercoiling determination

Global DNA supercoiling was assayed in bacterial strains transformed with a reporter plasmid pUC18. An overnight culture of pUC18-containg strain was adjusted to an OD_{600} of 0.003 and grown to the late stationary growth stage (24 h) in 25 ml LB broth or in 25 ml of minimal medium N of the required $MgCl_2$ concentration pre-conditioned as above. Fourteen OD_{600} units (6 OD_{600} units for minimal medium) were harvested and pUC18 was isolated with the aid the of QIAprep Spin miniprep kit (QIAGEN, Hilden, Germany) according to manufacturer's guidelines.

To observe the range of DNA supercoiling states characteristic of a strain at a given growth stage, extracted pUC18 samples were resolved on 0.8% agarose gel supplemented with the DNA intercalating agent chloroquine. 2 L of 1x TBE buffer (89 mM Tris base, 89 mM boric acid, 2 mM EDTA pH 8.0) and 1 ml of 25 mg/ml chloroquine were made. 0.8% agarose solution was made from 300 µl TBE and melted in a Tyndall steamer. When the gel cooled down, it was supplemented with 2.5 µg/ml chloroquine. The 27 cm long gel was poured, left to polymerise for 2 h and covered with 1.7 litres of the running buffer containing 1x TBE and chloroquine at 2.5 µg/ml. 1 µg or 500 ng of the plasmid samples in 15 µl volumes were mixed with 5x loading dye (80% glycerol, 0.01% bromophenol blue) and loaded on a gel. The gel was electrophoresed for 16 h at 100 V. The gel was washed in distilled water for 24 h changing water a few times, stained in 1 µg/ml ethidium bromide for 1 h rocking in the dark. The stain was poured off and the gel was washed in distilled water for further 1 h. The plasmid topoisomers were visualised under UV on the ImageQuant LAS 4000 imager. ImageJ software was used to outline plasmid topoisomer distribution profiles.

Determining the patterns of gyrA *and* gyrB *locations in bacterial chromosomes*

The location of *oriC* in each organism examined was determined using the DoriC 10.0 database (tubic.org/doric) (Luo and Gao, 2019) and the coordinates of their *gyrA* and *gyrB* genes were obtained using the Ensembl bacteria browser (bacteria.ensembl.org). Distance in base pairs between the

oriC and the gene was calculated and converted into the percentage of the total chromosome size. An attempt was made to cover bacterial taxonomy as broadly as possible, encompassing members of the major bacterial phyla, well studied, and clinically important organisms in the analysis (Table 1). The table is neither complete nor does it claim to include all the existing possibilities of *gyrA* and *gyrB* arrangements in bacterial chromosomes, but instead, exemplifies the arrangement possibilities mentioned in this work. Closely related species and those belonging to the less diverse phyla were found to share the chromosomal positions of *gyrA* and *gyrB* frequently. Thus, one representative of a taxonomic rank was often deemed sufficient for the purpose of inclusion in the table. Lower classification ranks were analysed within more diverse and studied phyla.

Mammalian cell culture conditions

RAW264.7 murine macrophages were maintained in Dulbecco's Modified Eagle's Medium (DMEM), (Sigma, catalogue number D6429) supplemented with 10% fetal bovine serum (FBS) in a humidified 37°C, 5% CO_2 tissue-culture incubator grown in 75 cm^3 tissue-culture flasks. When approximately 80% confluent growth was achieved, cells were split to a fresh flask. Cells within the 9-16 passage number range were used for infections. All media and PBS used for cell culture were pre-warmed to 37°C. To split cells, old DMEM was removed and the monolayer was rinsed with 10 ml of sterile PBS. Ten ml of fresh DMEM was pipetted into the flask and the monolayer was scraped gently with a cell scraper to dislodge the cells. Scraped cells were centrifuged at 450 x g for 5 min in an Eppendorf 5810R centrifuge and the cell pellet was resuspended in 5 ml DMEM+FBS. One ml of the cell suspension was added to 14 ml of fresh DMEM+FBS in a 75 cm^3 flask, gently rocked to mix and incubated at 37°C, 5% CO_2. To seed cells for infection, cells were treated as for splitting. After resuspension in 5 ml DMEM+FBS, viable cells were counted on a haemocytometer using trypan blue exclusion dye. A 24-well tissue culture plate was filled with 500 µl DMEM+FBS. 1.5×10^5 cells were added to each well, gently rocked to mix and incubated at 37°C, 5% CO_2 for 24 h.

Macrophage viability assay in SPI-1 inducing conditions

Overnight bacterial cultures were subcultured 1:33 in 10 ml of fresh LB broth in 125 ml conical flask and grown for 3.5 h to maximize SPI-1 expression (Steele-Mortimer *et al.*, 1999). 500 µl of the culture was centrifuged at 16000 x g for 1 min and resuspended in 500 µl of HBSS-/-. Monolayers were washed twice with 500 µl of HBSS+/+ and infected with bacteria at MOI of 5 in three technical replicates for each timepoint and strain. The plate was centrifuged at 200 x g for 10 min to synchronize infections and incubated for 30 min at 37°C, 5% CO_2. In the meantime, the infection medium was plated for enumeration on LB agar plates – T=0 h. Gentamycin protection assay was used to determine bacterial counts inside macrophages. To kill all extracellular bacteria, the monolayers were washed once with HBSS+/+ and high gentamycin (100 µg/ml) treatment diluted in DMEM+FBS was added to the wells. The plate was incubated at 37°C, 5% CO_2 for 1 h. At 1 h post infection the monolayers were washed three times with HBSS+/+, macrophages were lysed by adding 1 ml of ice-cold water, pipetting up and down ten times with scraping and intracellular bacteria were plated for enumeration. The monolayers which were intended for other timepoints, were washed once with HBSS+/+, low gentamycin (10 µg/ml) treatment in DMEM+FBS was added and the plate was incubated at 37°C, 5% CO_2. The low gentamycin concentration is to ensure that any extracellular bacteria are killed, but at the same time to avoid gentamycin permeabilizing plasma membrane of a macrophage (Kaneko *et al.*, 2016). At later timepoints monolayers were washed three times with HBSS+/+, macrophages were lysed by adding 1 ml ice-cold water, pipetting up and down ten times with scraping and intracellular bacteria were plated for enumeration.

Acknowledgements

Research in the CJD laboratory is supported by Science Foundation Ireland Investigator Award 13/IA/1875.

Conflicts of interest

The authors declare that they have no conflicts of interest.

References

Ahmed, W., Menon, S., Karthik, P.V., and Nagaraja, V. (2016) Autoregulation of topoisomerase I expression by supercoiling sensitive transcription. *Nucleic Acids Res* **44:** 1541-1552.

Ahmed, W., Sala, C., Hegde, S.R., Jha, R.K., Cole, S.T., and Nagaraja, V. (2017) Transcription facilitated genome-wide recruitment of topoisomerase I and DNA gyrase. *PLoS Genet* **13:** 1-20.

Alokam, S., Liu, S.L., Said, K., and Sanderson, K.E. (2002) Inversions over the terminus region in *Salmonella* and *Escherichia coli*: IS*200*s as the sites of homologous recombination inverting the chromosome of *Salmonella enterica* serovar Typhi. *J Bacteriol* **184**: 6190-6197.

Ashley, R.E., Dittmore, A., McPherson, S.A., Turnbough, C.L. Jr., Neuman, K.C., and Osheroff, N. (2017) Activities of gyrase and topoisomerase IV on positively supercoiled DNA. *Nucleic Acids Res* **45:** 9611-9624.

Baba, T., Ara, T., Hasegawa, M., Takai, Y., Okumura, Y., Baba, M., Datsenko, K.A., Tomita, M., Wanner, B.L., and Mori, H. (2006) Construction of *Escherichia coli* K-12 in-frame, single-gene knockout mutants: the Keio collection. *Mol Syst Biol* **2**: 2006.0008.

Baba, T., Bae, T., Schneewind, O., Takeuchi, F., and Hiramatsu, K. (2008) Genome sequence of *Staphylococcus aureus* strain Newman and comparative analysis of Staphylococcal genomes; polymorphism and evolution of two major pathogenicity islands. *J Bacteriol* **190:** 300-310.

Banda, M.M., Zavala-Alvarado, C., Perez-Morales, D., Bustamante, V.H. (2019) SlyA and HilD counteract H-NS-mediated repression on the *ssrAB* virulence operon of *Salmonella enterica* serovar Typhimurium and thus promote its activation by OmpR. *J Bacteriol* **201:** e00530-18.

Bates, A.D., and Maxwell, A. (2005) *DNA Topology*. Oxford University Press.

Berger, J.M. (1998) Type II DNA topoisomerases. *Curr Opin Struct Biol* **8:** 26-32.

Berlyn, M.K. (1998) Linkage map of *Escherichia coli* K-12, edition 10: the traditional map. *Microbiol Mol Biol Rev* **62:** 814-984.

Blattner, F.R., Plunkett, G., III, Bloch, C.A., Perna, N.T., Burland, V., Riley, M., Collado-Vides, J., Glasner, J.D., Rode, C.K., Mayhew, G.F., Gregor, J.,

886 Davis, N.W., Kirkpatrick, H.A., Goeden, M.A., Rose, D.J., Mau, B., and
887 Shao, Y. 1997. The complete genome sequence of *Escherichia coli* K-12.
888 *Science* **277:** 1453-1474.
889 Bliska, J.B., and Cozzarelli, N.R. (1987) Use of site-specific recombination as
890 a probe of DNA structure and metabolism *in vivo. J Mol Biol* **194:** 205-218.
891 Bogue, M.M., Mogre, A., Beckett, M.C., Thomson, N.R., and Dorman, C.J.
892 (2020) Network rewiring: physiological consequences of reciprocally
893 exchanging the physical locations and growth-phase-dependent expression
894 patterns of the *Salmonella fis* and *dps* genes. *mBio* **11**: e0218-20.
895 Bryant, J.A., Sellars, L.E., Busby, S.J., and Lee, D.J. (2014) Chromosome
896 position effects on gene expression in *Escherichia coli* K-12. *Nucleic Acids*
897 *Res* **42:** 11383-11392.
898 Bush, N.G., Diez-Santos, I., Abbott, L.R., and Maxwell, A. (2020) Quinolones:
899 mechanism, lethality and their contributions to antibiotic resistance.
900 *Molecules* **25:** 5662.
901 Cameron, A.D., and Dorman, C.J. (2012) A fundamental regulatory
902 mechanism operating through OmpR and DNA topology controls
903 expression of *Salmonella* pathogenicity islands SPI-1 and SPI-2. *PLoS*
904 *Genet* **8**: e1002615.
905 Cameron, A.D., Stoebel, D.M., and Dorman, C.J. (2011) DNA supercoiling is
906 differentially regulated by environmental factors and FIS in *Escherichia coli*
907 and *Salmonella enterica. Mol Microbiol* **80:** 85-101.
908 Champion, K., and Higgins, N.P. (2007) Growth rate toxicity phenotypes and
909 momeostatic supercoil control differentiate *Escherichia coli* from
910 *Salmonella enterica* serovar Typhimurium. *J Bacteriol* **189:** 5839-5849.
911 Cherepanov, P.P., and Wackernagel, W. (1995) Gene disruption in
912 *Escherichia coli*: TcR and KmR cassettes with the option of Flp-catalyzed
913 excision of the antibiotic-resistance determinant. *Gene* **158**: 9-14.
914 Cheung, K.J., Badarinarayana, V., Selinger, D.W., Janse, D., and Church,
915 G.M. (2003) A microarray-based antibiotic screen identifies a regulatory
916 role for supercoiling in the osmotic stress response of *Escherichia coli*.
917 *Genome Res* **13:** 206-215.
918 Chong, S., Chen, C., Ge, H., and Xie, X.S. (2014) Mechanism of

transcriptional bursting in bacteria. *Cell* **158:** 314-326.
Colgan, A.M., Quinn, H.J., Kary, S.C., Mitchenall, L.A., Maxwell, A., Cameron, A.D.S., and Dorman, C.J. (2018) Negative supercoiling of DNA by gyrase is inhibited in *Salmonella enterica* serovar Typhimurium during adaptation to acid stress. *Mol Microbiol* **107:** 734-746.
Conter, A., Menchon, C., and Gutierrez, C. (1997) Role of DNA supercoiling and *rpoS* sigma factor in the osmotic and growth phase-dependent induction of the gene *osmE* of *Escherichia coli* K12. *J Mol Biol* **273:** 75-83.
Cooper, S., and Helmstetter, C.E. (1968) Chromosome replication and the division cycle of *Escherichia coli* B/r. *J Mol Biol* **31:** 519-540.
Corbett, K.D., and Berger, J.M. (2004) Structure, molecular mechanisms, and evolutionary relationships in DNA topoisomerases. *Annu Rev Biophys Biomol Struct* **33:** 95-118.
Dandekar, T., Snel, B., Huynen, M., and Bork, P. (1998) Conservation of gene order: A fingerprint of proteins that physically interact. *Trends Biochem Sci* **23:** 324-328.
Deatherage, D.E., and Barrick, J.E. (2014) Identification of mutations in laboratory-evolved microbes from next-generation sequencing data using breseq. *Methods Mol Biol* **1151**: 165-188.
de Daruvar, A., Collado-Vides, J., and Valencia, A. (2002) Analysis of the cellular functions of *Escherichia coli* operons and their conservation in *Bacillus subtilis. J Mol Evol* **55:** 211-221.
Dekker, N.H., Rybenkov, V.V., Duguet, M., Crisona, N.J., Cozzarelli, N.R., Bensimon, D., and Croquette, V. (2002) The mechanism of type IA topoisomerases. *Proc Natl Acad Sci USA* **99:** 12126-12131.
Dillon, S.C., and Dorman, C.J. (2010) Bacterial nucleoid-associated proteins, nucleoid structure and gene expression. *Nat Rev Microbiol* **8:** 185-195.
DiNardo, S., Voelkel, K.A., Sternglanz, R., Reynolds, A.E., and Wright, A. (1982) *Escherichia coli* DNA topoisomerase I mutants have compensatory mutations in DNA gyrase genes. *Cell* **31:** 43-51.
Dorman, C.J. (2019) DNA supercoiling and transcription: a two-way street. *BMC Mol Cell Biol* **20:** 26-39.
Dorman, C.J., and Dorman, M.J. (2016) DNA supercoiling is a fundamental

952 regulatory principle in the control of bacterial gene expression. *Biophys Rev*
953 **8:** 209-220.
954 Dorman, C.J., Lynch, A.S., Ní Bhriain, N., and Higgins, C.F. (1989) DNA
955 supercoiling in *Escherichia coli*: *topA* mutations can be suppressed by DNA
956 amplifications involving the *tolC* locus. *Mol Microbiol* **3:** 531-540.
957 Drlica, K., and Zhao, X. (1997) DNA gyrase, topoisomerase IV, and the 4-
958 quinolones. *Microbiol Mol Biol Rev* **61**: 377-392.
959 Fass, E., and Groisman, E.A. (2009) Control of *Salmonella* pathogenicity
960 island-2 gene expression. *Curr Opin Microbiol* **12:** 199-204
961 Figueira, R., and Holden, D.W. (2012) Functions of the *Salmonella*
962 pathogenicity island 2 (SPI-2) type III secretion system effectors.
963 *Microbiology* **158:** 1147-1161.
964 Forterre, P., Gribaldo, S., Gadelle, D., and Serre, M.C. (2007) Origin and
965 evolution of DNA topoisomerases. *Biochimie* **89:** 427-446.
966 Garvis, S.G., Beuzón, C.R., and Holden, D.W. (2001) A role for the PhoP/Q
967 regulon in inhibition of fusion between lysosomes and *Salmonella*-
968 containing vacuoles in macrophages. *Cell Microbiol* **3:** 731-744.
969 Gellert, M., Mizuuchi, K., O'Dea, M.H., and Nash, H.A. (1976a) DNA gyrase:
970 enzyme that introduces superhelical turns into DNA. *Proc Natl Acad Sci*
971 *USA* **73:** 3872–3876.
972 Gellert, M., Mizuuchi, K., O'Dea, M.H., Itoh, T., and Tomizawa, J.I. (1977)
973 Nalidixic acid resistance: a second genetic character involved in DNA
974 gyrase activity. *Proc Natl Acad Sci USA* **74:** 4772–4776.
975 Gerganova, V., Berger, M., Zaldastanishvili, E., Sobetzko, P., Lafon, C.,
976 Mourez, M., Travers, A., and Muskhelishvili, G. (2015) Chromosomal
977 position shift of a regulatory gene alters the bacterial phenotype. *Nucleic*
978 *Acids Res* **43:** 8215-8226.
979 Glaser, P., Frangeul, L., Buchrieser, C., Rusniok, C., Amend, A., Baquero, F.,
980 Berche, P., Bloecker, H., Brandt, P., Chakraborty, T., Charbit, A.,
981 Chetouani, F., Couvé, E., de Daruvar, A., Dehoux, P., Domann, E.,
982 Domínguez-Bernal, G., Duchaud, E., Durant, L., Dussurget, O., Entian,
983 K.D., Fsihi, H., García-del Portillo, F., Garrido, P., Gautier, L., Goebel, W.,
984 Gómez-López, N., Hain, T., Hauf, J., Jackson, D., Jones, L.M., Kaerst, U.,

985 Kreft, J., Kuhn, M., Kunst, F., Kurapkat, G., Madueno, E., Maitournam, A.,
986 Vicente, J.M., Ng, E., Nedjari, H., Nordsiek, G., Novella, S., de Pablos, B.,
987 Pérez-Diaz, J.C., Purcell, R., Remmel, B., Rose, M., Schlueter, T., Simoes,
988 N., Tierrez, A., Vázquez-Boland, J.A., Voss, H., Wehland, J., and Cossart,
989 P. (2001) Comparative genomics of *Listeria* species. *Science* **294:** 849-
990 852.
991 Hensel, M. (2000) *Salmonella* pathogenicity island 2. *Mol Microbiol* **36:** 1015-
992 1023.
993 Higgins, N.P. (2014) RNA polymerase: chromosome domain boundary maker
994 and regulator of supercoil density. *Curr Opin Microbiol* **22:** 138-143.
995 Higgins, N.P. (2016) Species-specific supercoil dynamics of the bacterial
996 nucleoid. *Biophys Rev* **8:** 113-121.
997 Higgins, N.P., Peebles, C.L., Sugino, A., and Cozzarelli, N.R. (1978)
998 Purification of subunits of *Escherichia coli* DNA gyrase and reconstitution of
999 enzymatic activity. *Proc Natl Acad Sci USA* **75:** 1773-1777.
1000 Hoiseth, S.K., and Stocker, B.A. (1981) Aromatic-dependent *Salmonella*
1001 Typhimurium are non-virulent and effective as live vaccines. *Nature* **291**:
1002 238-239.
1003 Ibarra, J.A., Knodler, L.A., Sturdevant, D.E., Virtaneva, K., Carmody, A.B.,
1004 Fischer, E.R., Porcella, S.F., and Steele-Mortimer, O. (2010) Induction of
1005 *Salmonella* pathogenicity island 1 under different growth conditions can
1006 affect *Salmonella*-host cell interactions *in vitro*. *Microbiology* **156**: 1120-
1007 1133.
1008 Kaneko, M., Emoto, Y., and Emoto, M. (2016) A simple, reproducible,
1009 inexpensive, yet old-fashioned method for determining phagocytic and
1010 bactericidal activities of macrophages. *Yonsei Med J* **57**: 283-290.
1011 Keane, O.M., and Dorman, C.J. (2003) The *gyr* genes of *Salmonella enterica*
1012 serovar Typhimurium are repressed by the factor for inversion stimulation,
1013 Fis. *Mol Genet Genomics* **270**: 56-65.
1014 Klostermeier, D. (2018) Why two? On the role of (A-)symmetry in negative
1015 supercoiling of DNA by gyrase. *Int J Mol Sci* **19:** 1489
1016 Lacharme-Lora, L., Owen, S.V., Blundell, R., Canals, R., Wenner, N., Perez-
1017 Sepulveda, B., Fong, W.Y., Gilroy, R., Wigley, P., and Hinton, J.C.D.

(2019) The use of chicken and insect infection models to assess the virulence of African *Salmonella* Typhimurium ST313. *PLoS Negl Trop Dis* **13:** e0007540.

Lawrence, J.G., and Roth, J.R. (1996) Selfish operons: horizontal transfer may drive the evolution of gene clusters. *Genetics* **143:** 1843-1860.

Le, T.B., Laub, M.T. (2016) Transcription rate and transcript length drive formation of chromosomal interaction domain boundaries. *EMBO J* **35:** 1582-1595.

Letunic, I., and Bork, P. (2019) Interactive Tree Of Life (iTOL) v4: recent updates and new developments. *Nucleic Acids Res* **47**: W256-w259.

Lewis, R.J., Singh, O.M., Smith, C.V., Skarzynski, T., Maxwell, A., Wonacott, A.J., and Wigley, D.B. (1996) The nature of inhibition of DNA gyrase by the coumarins and the cyclothialidines revealed by X-ray crystallography. *EMBO J* **15**: 1412-1420.

Li, G.W., Burkhardt, D., Gross, C., and Weissman, J.S. (2014) Quantifying absolute protein synthesis rates reveals principles underlying allocation of cellular resources. *Cell* **157:** 624-635.

Liu, L.F., and Wang, J.C. (1987) Supercoiling of the DNA template during transcription. *Proc Natl Acad Sci USA* **84:** 7024-7027.

Luo, H., and Gao, F. (2019) DoriC 10.0: an updated database of replication origins in prokaryotic genomes including chromosomes and plasmids. *Nucleic Acids Res* **47**: D74-D77.

McClelland, M., Sanderson, K.E., Spieth, J., Clifton, S.W., Latreille, P., Courtney, L., Porwollik, S., Ali, J., Dante, M., Du, F., Hou, S., Layman, D., Leonard, S., Nguyen, C., Scott, K., Holmes, A., Grewal, N., Mulvaney, E., Ryan, E., Sun, H., Florea, L., Miller, W., Stoneking, T., Nhan, M., Waterston, R., and Wilson, R.K. (2001) Complete genome sequence of *Salmonella enterica* serovar Typhimurium LT2. *Nature* **413:** 852-856.

Mangan, M.W., Lucchini, S., Danino, V., O Cróinín, T., Hinton, J.C., Dorman, C.J. (2006) The integration host factor (IHF) integrates stationary-phase and virulence gene expression in *Salmonella enterica* serovar Typhimurium. *Mol Microbiol* **59:** 1831-1847.

Mangan, M.W., Lucchini, S., O Cróinín, T., Fitzgerald, S., Hinton, J.C.,

1051 Dorman, C.J. (2011) Nucleoid-associated protein HU controls three
1052 regulons that coordinate virulence, response to stress and general
1053 physiology in *Salmonella enterica* serovar Typhimurium. *Microbiology* **157:**
1054 1075-1087.
1055 Martín CM, Zaritsky A, Fishov I, and Guzmán EC. (2020) Transient enhanced
1056 cell division by blocking DNA synthesis in *Escherichia coli. Microbiology*
1057 **166:** 516-521.
1058 Mansour, F.H., and Pestov, D.G. (2013) Separation of long RNA by agarose-
1059 formaldehyde gel electrophoresis. *Anal Biochem* **441**: 18-20.
1060 Menzel, R., and Gellert, M. (1983) Regulation of the genes for *E. coli* DNA
1061 gyrase: homeostatic control of DNA supercoiling. *Cell* **34:** 105-113.
1062 Menzel, R., and Gellert, M. (1987) Modulation of transcription by DNA
1063 supercoiling: a deletion analysis of the *Escherichia coli gyrA* and *gyrB*
1064 promoters. *Proc Natl Acad Sci USA* **84:** 4185-4189.
1065 Miller, J.F. (1972) *Experiments in Molecular Genetics.* Cold Spring Harbor
1066 Laboratory Press, Cold Spring Harbor, New York.
1067 Moffitt, J.R., Pandey, S., Boettiger, A.N., Wang, S., Zhuang, X. (2016) Spatial
1068 organization shapes the turnover of a bacterial transcriptome. *eLife* **5**:
1069 e13065
1070 Nelson, D.L., and Kennedy, E.P. (1971) Magnesium transport in *Escherichia*
1071 *coli.* Inhibition by cobaltous ion. *J Biol Chem* **246:** 3042-304
1072 Neumann, S., and Quiñones, A. (1997) Discoordinate gene expression of
1073 *gyrA* and *gyrB* in response to DNA gyrase inhibition in *Escherichia coli*. *J*
1074 *Basic Microbiol* **37**: 53-69.
1075 Nöllmann, M., Stone, M.D., Bryant, Z., Gore, J., Crisona, N.J., Hong, S.-C.,
1076 Mitelheiser, S., Maxwell, A., Bustamante, C., and Cozzarelli, N.R. (2007)
1077 Multiple modes of *Escherichia coli* DNA gyrase activity revealed by force
1078 and torque. *Nat Struct Mol Biol* **14:** 264-271.
1079 O Cróinín, T., Carroll, R.K., Kelly, A., and Dorman, C.J. (2006) Roles for DNA
1080 supercoiling and the Fis protein in modulating expression of virulence
1081 genes during intracellular growth of *Salmonella enterica* serovar
1082 Typhimurium. *Mol Microbiol* **62**: 869-882.
1083 Pal. C., and Hurst. L.D. (2004) Evidence against the selfish operon theory.

Trends Genet **20:** 232–234.

Peter, B.J., Arsuaga, J., Breier, A.M., Khodursky, A.B., Brown, P.O., and Cozzarelli, N.R. (2004) Genomic transcriptional response to loss of chromosomal supercoiling in *Escherichia coli. Genome Biol* **5:** R87.

Price, M.N., Huang, K.H., Alm, E.J., and Arkin, A.P. (2005) Operon formation is driven by co-regulation and not by horizontal gene transfer. *Genome Res* **15:** 809-819.

Price, M.N., Arkin, A.P., and Alm, E.J. (2006) The life-cycle of operons. *PLoS Genet* **2:** e96.

Pruss, G.J., Manes, S.H., and Drlica, K. (1982) *Escherichia coli* DNA topoisomerase I mutants: increased supercoiling is corrected by mutations near gyrase genes. *Cell* **31:** 35-42.

Quinn, H.J., Cameron, A.D., and Dorman, C.J. (2014) Bacterial regulon evolution: distinct responses and roles for the identical OmpR proteins of *Salmonella* Typhimurium and *Escherichia coli* in the acid stress response. *PLoS Genet* **10**: e1004215.

Rahmouni, A.R., and Wells, R.D. (1992) Direct evidence for the effect of transcription on local DNA supercoiling *in vivo. J Mol Biol* **223:** 131-144.

Raji, A., Zabel, D.J., Laufer, C.S., and Depew, R.E. (1985) Genetic analysis of mutations that compensate for loss of *Escherichia coli* DNA topoisomerase I. *J Bacteriol* **162:** 1173-1179.

Rani, P., and Nagaraja, V. (2019) Genome-wide mapping of Topoisomerase I activity sites reveal its role in chromosome segregation. *Nucleic Acids Res* **47:** 1416-1427.

Richardson, S.M., Higgins, C.F., and Lilley, D.M. (1988) DNA supercoiling and the *leu-500* promoter mutation of *Salmonella typhimurium*. *EMBO J* **7:** 1863-1869.

Rocha, E.P. (2008) The organization of the bacterial genome. *Annu Rev Genet* **42**: 211-233.

Rogozin, I.B., Makarova, K.S., Murvai, J., Czabarka, E., Wolf, Y.I., Tatusov, R.L., Szekely, L.A., and Koonin, E.V. (2002) Connected gene neighborhoods in prokaryotic genomes. *Nucleic Acids Res* **30:** 2212-2223.

Sambrook, J., and Russell, D.W. (2006) Purification of nucleic acids by

1117 extraction with phenol:chloroform. *CSH Protoc* **2006**.
1118 Schmieger, H. (1972) Phage P22-mutants with increased or decreased
1119 transduction abilities. *Mol Gen Genet* **119**: 75-88.
1120 Schneider, R., Travers, A., Kutateladze, T., and Muskhelishvili, G. (1999) A
1121 DNA architectural protein couples cellular physiology and DNA topology in
1122 *Escherichia coli*. *Mol Microbiol* **34**: 953-964.
1123 Scholz, S.A., Diao, R., Wolfe, M.B., Fivenson, E.M., Lin, X.N., and Freddolino,
1124 P.L. (2019) High-resolution mapping of the *Escherichia coli* chromosome
1125 reveals positions of high and low transcription. *Cell Syst* **8:** 212-225.
1126 Sharma, B., and Hill, T.M. (1995) Insertion of inverted Ter sites into the
1127 terminus region of the *Escherichia coli* chromosome delays completion
1128 of DNA replication and disrupts the cell cycle. *Mol Microbiol* **18:** 45-61.
1129 Sobetzko, P. (2016) Transcription-coupled DNA supercoiling dictates the
1130 chromosomal arrangement of bacterial genes. *Nucleic Acids Res* **44**: 1514-
1131 1524.
1132 Sobetzko, P., Travers, A., and Muskhelishvili, G. (2012) Gene order and
1133 chromosome dynamics coordinate spatiotemporal gene expression during
1134 the bacterial growth cycle. *Proc Natl Acad Sci USA* **109:** E42-E50.
1135 Steck, T.R., Pruss, G.J., Manes, S.H., Burg, L., and Drlica, K. (1984) DNA
1136 supercoiling in gyrase mutants. *J Bacteriol* **158:** 397-403.
1137 Steele-Mortimer, O., Méresse, S., Gorvel, J.P., Toh, B.H., and Finlay, B.B.
1138 (1999) Biogenesis of *Salmonella* Typhimurium-containing vacuoles in
1139 epithelial cells involves interactions with the early endocytic pathway. *Cell*
1140 *Microbiol* **1**: 33-49.
1141 Stracy, M., Wollman, A.J.M., Kaja, E., Gapinski, J., Lee, J.E., Leek, V.A.,
1142 McKie, S.J., Mitchenall, L.A., Maxwell, A., Sherratt, D.J., Leake, M.C., and
1143 Zawadzki, P. (2019) Single-molecule imaging of DNA gyrase activity in
1144 living *Escherichia coli. Nucleic Acids Res* **47:** 210-220.
1145 Straney, R., Krah, R., and Menzel, R. (1994) Mutations in the -10 TATAAT
1146 sequence of the *gyrA* promoter affect both promoter strength and sensitivity
1147 to DNA supercoiling. *J Bacteriol* **176:** 5999-6006.
1148 Sutormin, D., Rubanova, N., Logacheva, M., Ghilarov, D., and Severinov, K.
1149 (2019) Single-nucleotide-resolution mapping of DNA gyrase cleavage sites

across the *Escherichia coli* genome. *Nucleic Acids Res* **47:** 1373-1388.
Swain, P.S. (2004) Efficient attenuation of stochasticity in gene expression through post-transcriptional control. *J Mol Biol* **344:** 965-976.
Tobe T., Yoshikawa, M., and Sasakawa, C. (1995) Thermoregulation of *virB* transcription in *Shigella flexneri* by sensing of changes in local DNA superhelicity. *J Bacteriol* **177:** 1094-1097.
Tse-Dinh, Y., and Beran, R. (1988) Multiple promoters for transcription of the *E. coli* DNA topoisomerase I gene and their regulation by DNA supercoiling. *J Mol Biol* **202:** 735-742.
Unniraman, S., and Nagaraja, V. (1999) Regulation of DNA gyrase operon in *Mycobacterium smegmatis*: a distinct mechanism of relaxation stimulated transcription. *Genes Cells* **4:** 697-706.
Unniraman, S., Chatterji, M., and Nagaraja, V. (2002) DNA gyrase in *Mycobacterium tuberculosis*: a single operon driven by multiple promoters. *J Bacteriol* **184:** 5449-5456.
van der Heijden, J., and Finlay, B.B. (2012) Type III effector-mediated processes in *Salmonella* infection. *Future Microbiol* **7:** 685-703.
Weidlich, D., and Klostermeier, D. (2020) Functonal interactions between gyrase subunits are optimized in a species-specific manner. *J Biol Chem* **295:** 22299-2312.
Williams, N.L., and Maxwell, A. (1999) Probing the two-gate mechanism of DNA gyrase using cysteine cross-linking. *Biochemistry* **38:** 13502-13511.
Wu, H.Y., Shyy, S.H., Wang, J.C., and Liu, L.F. (1988) Transcription generates positively and negatively supercoiled domains in the template. *Cell* **53:** 433-440.
Yanisch-Perron, C., Vieira, J., and Messing, J. (1985) Improved M13 phage cloning vectors and host strains: nucleotide sequences of the M13mp18 and pUC19 vectors. *Gene* **33**: 103-119.
Zerbino, D.R. (2010) Using the Velvet *de novo* assembler for short-read sequencing technologies. *Curr Protoc Bioinformatics* **Chapter 11**: Unit 11.15.

1183 **Table 1.** Relative positions of *gyrB* and *gyrA* across bacterial species

Organism (phylum, lowest clade sharing the arrangement)	***gyrB* to *oriC* distance in bp, Left or Right replichore**	***gyrB* to *oriC* distance as % total chromo-some**	***gyrA* to *oriC* distance in bp, Left or Right replichore***	***gyrA* to *oriC* distance as % total chromo-some**
Group 1 (*gyrB* and *gyrA* positioned separately, *gyrB* near *oriC***)**				
Escherichia coli	45409, Right	0.98%	1585679, Right	34.20%
Salmonella enterica serovar Typhimurium	42033, Left	0.86%	1730509, Left	35.48%
Salmonella enterica serovar Gallinarum	37634, Right	0.81%	1382662, Left	29.68%
Shigella flexneri	57368, Left	1.25%	1577518, Left	34.24%
Yersinia pestis	37176, Left	0.79%	1073028, Right	22.82%
Vibrio cholerae	10386, Right	0.35%	1329436, Right	44.90%
Pseudomonas aeruginosa	2248, Right	0.04%	2708909, Left	43.26%
Xanthomonas axonopodis (all above are Proteobacteria, class Gammaproteobacteria)	3161, Right	0.06%	1876940, Right	36.27%
Azospirillum sp. (Proteobacteria (α), order Rhodospirillales)	179561, Left	5.42%	1595259, Right	48.17%
Caulobacter crescentus (Proteobacteria (α), order Caulobacterales)	166112, Right	4.14%	1744542, Right	43.43%
Azoarcus sp. (Proteobacteria (β), order Rhodocyclales)	32299, Right	0.61%	1182414, Left	22.49%
Burkholderia cepacia (Proteobacteria (β), Burkholderiales)	160154, Right	4.62%	859834, Left	24.82%
Campylobacter jejuni (Proteobactria, class Epsilonproteobacteria)	635, Right	0.04%	653170, Left	40.12%
Group 2 (*gyrB* and *gyrA* positioned separately, *gyrB* position variable**)**				
Myxococcus xanthus (Proteobacteria (Δ), order Myxococcales)	310304, Right	3.40%	872133, Right	9.54%
Bacteroides thetaiotaomicron (Bacteroidetes, family *Bacteroidaceae*)	246107, Right	3.93%	2199265, Left	35.10%
Bacteroides fragilis (Bacteroidetes, family *Bacteroidaceae*)	155636, Right	2.99%	2420574, Left	46.50%
Rickettsia prowazekii (Proteobacteria (α), order Rickettsiales)	382412, Left	34.40%	250129, Right	22.50%
Neisseria gonorrhoeae	412632, Left	19.16%	616174,	28.61%

(Proteobacteria (β), order Neisseriales)			Right	
Streptococcus pneumoniae (Firmicutes, family *Streptococcaceae*)	786742, Left	37.25%	951471, Right	45.05%
Streptococcus pyogenes (Firmicutes, family *Streptococcaceae*)	521569, Left	27.53%	897992, Right	47.40%
Flavobacterium columnare (Bacteroidetes, class Flavobacteria)	448681, Left	14.19%	1240595, Right	39.22%
Prevotella intermedia (Bacteroidetes, family *Prevotellaceae)*	267997, Left	12.64%	697114, Right	32.89%
Sphingobacterium sp. (Bacteroidetes, class Sphingobacteriia)	2928149, Right	47.03%	2182864, Left	35.06%
Porphyromonas gingivalis (Bacteroidetes, family *Porphyromonadaceae)*	552805, Left	23.59%	873251, Left	37.26%
Deinococcus radiodurans (Deinococcus-Thermus, class Deinococi)	911819, Right	34.45%	714641, Left	26.88%
Acidobacterium capsulatum (Acidobacteria, class Acidobacteria)	685949, Right	16.62%	33951, Left	0.82%

Group 3 (*gyrBA* operon near *oriC***)**

Geobacter sulfurreducens (Proteobacteria (Δ), order Desulfuromonadales)	1831, Right	0.05%	Downstream of *gyrB*
Pelobacter carbinolicus (Proteobacteria (Δ), order Desulfuromonadales)	2057, Right	0.06%	downstream of *gyrB*
Streptomyces coelicolor (Actinobacteria, class Actinobacteria)	3994, Left	0.05%	downstream of *gyrB*
Mycobacterium tuberculosis (Actinobacteria, class Actinobacteria)	2643, Right	0.06%	downstream of *gyrB*
Micrococcus luteus (Actinobacteria, family *Micrococcaceae*)	2843, Right	0.11%	downstream of *gyrB*
Clostridium tetani (Firmicutes, class Clostridia)	2472, Left	0.09%	downstream of *gyrB*
Lactobacillus brevis (Firmicutes, family *Lactobacillaceae*)	2557, Right	0.11%	downstream of *gyrB*
Enterococcus faecalis (Firmicutes, family *Enterococcaceae*)	5883, Right	0.20%	downstream of *gyrB*
Listeria monocytogenes (Firmicutes, order Bacillales)	3776, Right	0.13%	downstream of *gyrB*
Bacillus subtilis (Firmicutes, order Bacillales)	2546, Right	0.06%	downstream of *gyrB*
Spirochaeta thermophila (Spirochaetes, class Spirochaetia)	941, Left	0.38%	downstream of *gyrB*
Fusobacterium nucleatum (Fusobacteria, class Fusobacteriia)	3170, Left	0.15%	downstream of *gyrB*
Borrelia burgdorferi (Spirochaetes, class Spirochaetia)	1268, Left	0.14%	downstream of *gyrB*
Mycoplasma haemofelis (Tenericutes, class Mollicutes)	33798, Right	2.94%	downstream of *gyrB*

Group 4 *gyrBA* operon distant from *oriC*)

Chlamydia psittaci (Chlamydiae, class Chlamydiia)	573957, Left	48.97%	downstream of *gyrB*
Chlamydia trachomatis (Chlamydiae, class Chlamydiia)	504740, Left	48.42%	downstream of *gyrB*
Waddlia chondrophila (Chlamydiae, class Chlamydiia)	1044601, Right	49.36%	downstream of *gyrB*

*Where *gyrB* and *gyrA* form an operon, *gyrA* is universally located downstream of *gyrB*

1185 **Table 2.** Bacterial strains

Strain name	Genotype/ Description	Source/ reference
SL1344	*rpsL hisG*	Hoiseth and Stocker, 1981
SL1344 *gyrA*::*kan*	Kanamycin resistance cassette inserted downstream of the *gyrA* protein-coding region	This work
SL1344 *gyrB*::*kan*	Kanamycin resistance cassette inserted downstream of the *gyrB* protein-coding region	This work
SL1344 *gyrBA*	*gyrBA* operon under the control of the *gyrB* promoter, P_{gyrB}	This work
SL1344 *prgH*::*gfp*$^+$	*prgH-gfp*$^+$ [LVA]/R::*cat*/ fusion of a *gfp*$^+$ gene encoding a destabilised version of GFP to the SPI-1 promoter, P_{prgH}	Ibarra et al., 2010
SL1344 *gyrBA prgH*::*gfp*$^+$	Fusion of a *gfp*$^+$ derivative encoding a destabilised version of GFP to the SPI-1 promoter, P_{prgH} in the *gyrBA* background	This work
SL1344 *ssaG*::*gfp*$^+$	*prgH-gfp*$^+$ [LVA]/R::*cat*/ fusion of a *gfp*$^+$ derivative encoding a destabilised version of GFP to the SPI-2 promoter, P_{ssaG}	Ibarra et al., 2010
SL1344 *gyrBA ssaG*::*gfp*$^+$	Fusion of a *gfp*$^+$ derivative encoding a destabilised version of GFP to the SPI-2 promoter, P_{ssaG} in the *gyrBA* background	This work
SL1344 *SL1483*::*cat*	Insertion of a chloramphenicol resistance cassette into the pseudogene *SL1483*	This work
SL1344 *gyrBA SL1483*::*cat*	Insertion of a chloramphenicol resistance cassette into the pseudogene *SL1483* in the *gyrBA* background	This work

1186
1187

Table 3. Plasmids used in this study

Plasmid name	Description	Reference
pKD3	Amp^R ($Carb^R$), Cm^R	(Datsenko & Wanner, 2000)
pKD4	Amp^R ($Carb^R$), Kan^R	(Datsenko & Wanner, 2000)
pKD46	Amp^R ($Carb^R$), λ Red genes *γ, β, exo* under the control of an arabinose inducible promoter	(Datsenko & Wanner, 2000)
pCP20	Amp^R ($Carb^R$), Cm^R, FLP recombinase expressing, temperature sensitive replicon	(Cherepanov & Wackernagel, 1995)
pUC18	Amp^R ($Carb^R$),	(Yanisch-Perron *et al.*, 1985)

Abbreviations: Amp^R ($Carb^R$), ampicillin (carbenicillin) resistance; Cm^R, chloramphenicol resistance; Kan^R, kanamycin resistance.

Figures and legends

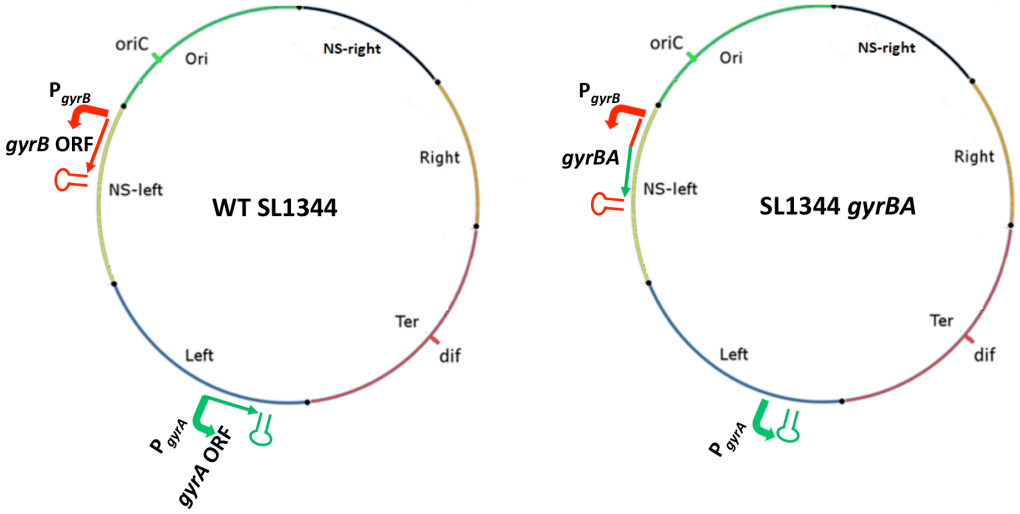

Fig. 1. Construction of a derivative of *S.* Typhimurium strain SL1344 with a *gyrBA* operon.

Chromosomal maps of the WT SL1344 and SL1344 *gyrBA* strains. Positions of *oriC*, *dif* and chromosome macrodomains are shown. Promoter (angled arrow), protein coding region (open reading frame, ORF) and the terminator (stem-loop structure) of the genes of interest are shown and colour coded. The *gyrA* ORF is green and the *gyrB* promoter and ORF are red. Not to scale.

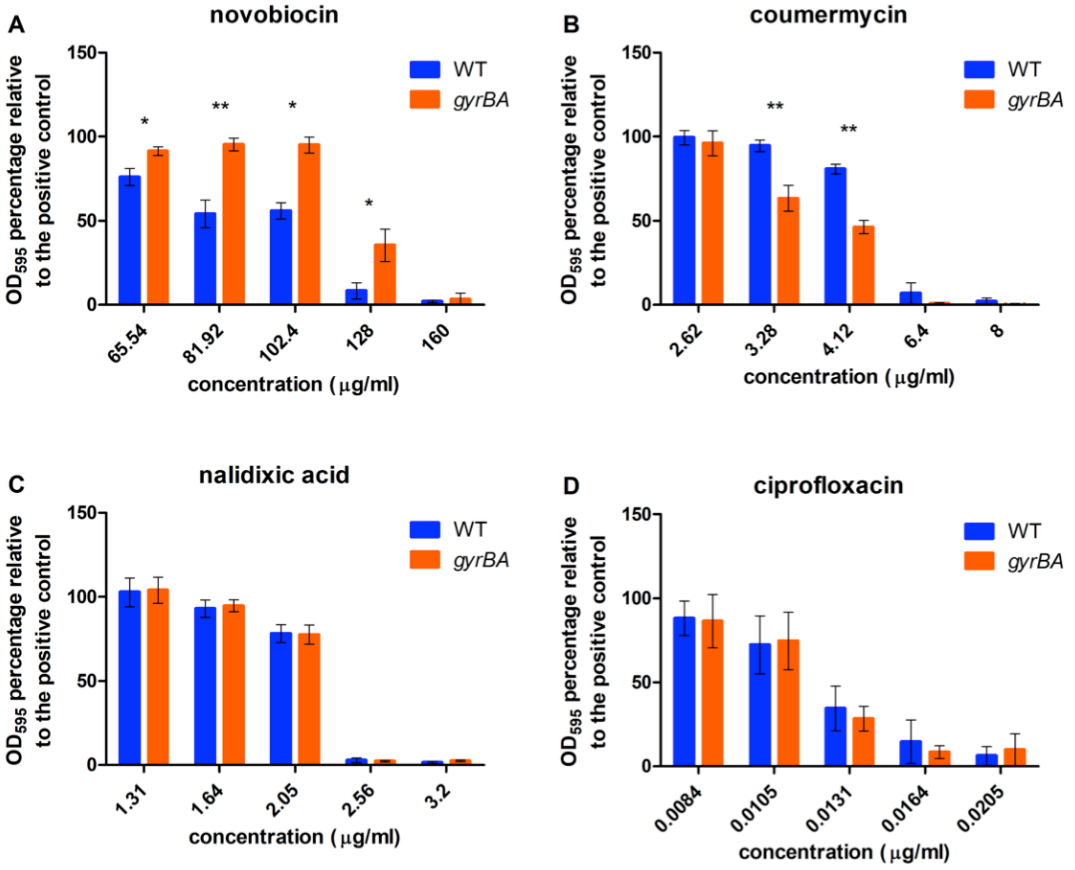

Fig. 2. Minimum inhibitory concentrations of DNA gyrase-inhibiting antibiotics in the wild type SL1344 and SL1344 *gyrBA* strains.

Cells were grown in a 96-well plate with 1:1.25 serially diluted antibiotics in LB broth for 18 h at 37°C and aeration. Cell density was measured by OD_{600}. A. Percentage survival of the WT and SL1344 *gyrBA* in 65.54-160 µg/ml novobiocin. MIC_{90} of the WT = 128 µg/ml, MIC_{90} of SL1344 *gyrBA* = 160 µg/ml. B. Percentage survival of the WT and the *gyrBA* in 2.62-8 µg/ml coumermycin, MIC_{90} = 6.4 µg/ml. C. Percentage survival of the WT and the *gyrBA* in 1.31 – 3.2 µg/ml nalidixic acid, MIC_{90} = 2.56 µg/ml. D. Percentage survival of the WT and the *gyrBA* in 0.0084 – 0.0205 µg/ml ciprofloxacin, MIC_{90} = 0.0164 µg/ml. Error bars represent the standard deviation of at least three biological replicates. Significance was found by unpaired Student's t-test, where * = P<0.05 and ** = P<0.01.

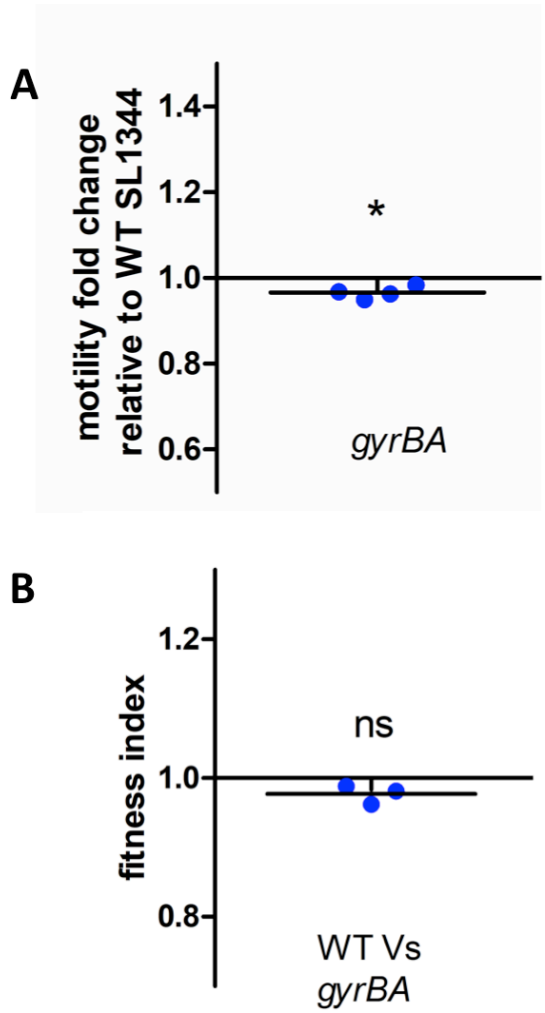

Fig. 3. Motility and competitive fitness of strain SL1344 *gyrBA*.
A. Diameters of swimming motility were measured after 5 h incubation at 37°C on soft 0.3% LB agar. The *gyrBA* strain is slightly, but statistically significantly, less motile than the WT. Values below 1 indicate that the strain is less motile than the WT. B) Fitness of the *gyrBA* strain was compared to the WT SL1344 in LB broth grown for 24 h with aeration at 37°C. Fitness index (f.i.) = 1 means that the competed strains were equally fit, f.i. < 1 indicates that the competitor strain is less fit than the WT, f.i. > 1 indicates that the competitor is more fit than the WT. The *gyrBA* and the WT were equally fit. Significance was determined by one sample T-test, where $P<0.05$.

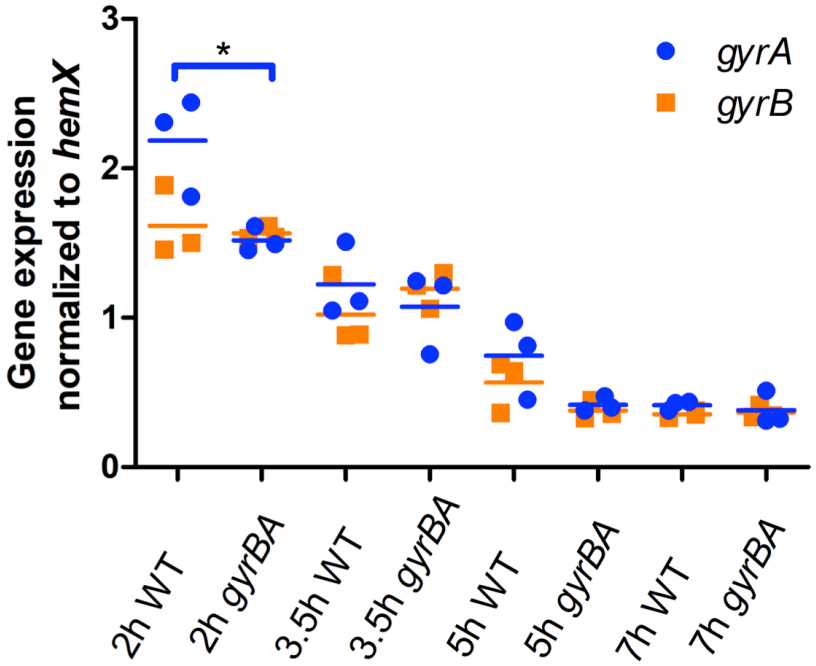

Fig. 4. Expression of the *gyrA* and *gyrB* genes in wild type SL1344 (WT) and SL1344 *gyrBA* during growth in liquid culture.
Cells were grown in LB broth at 37°C with aertion and samples were taken at 2 h, 3.5 h, 5 h and 7 h representing the lag, exponential, exponential-stationary transition and early stationary phases of growth, respectively. Transcription of *gyrA* and *gyrB* was measured and is reported relative to that of the *hemX* reference gene. Three biological replicates were used. Statistical significance was found by unpaired Student's T-test, where $P<0.05$.

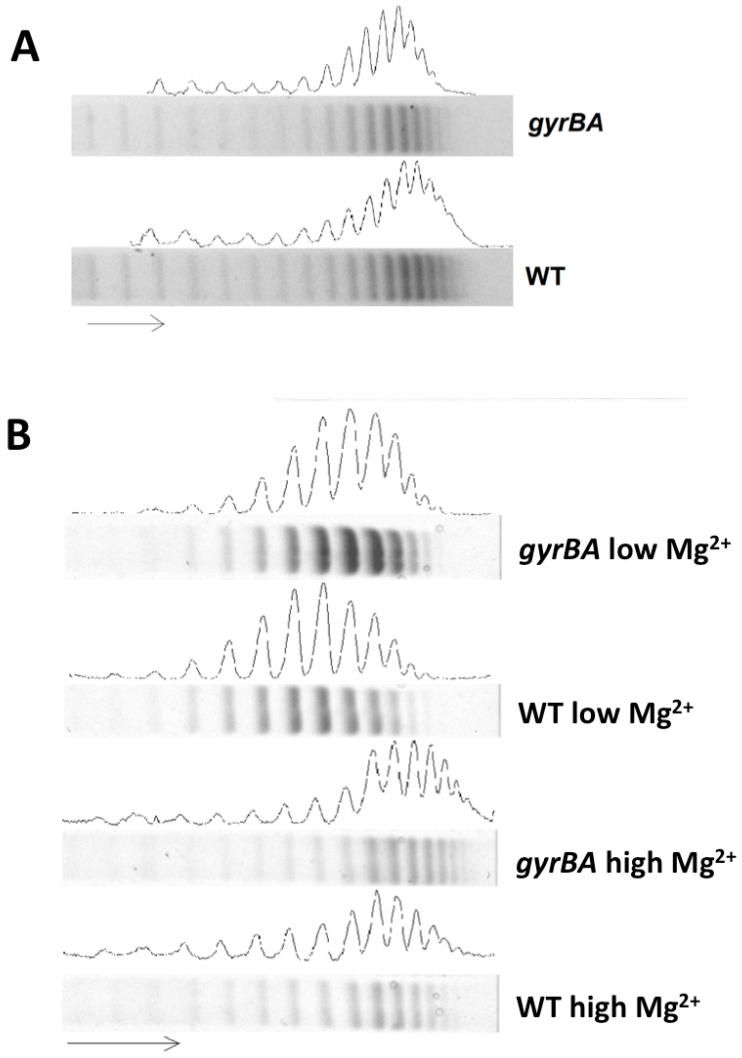

Fig. 5. Reporter plasmid DNA supercoiling in SL1344 *gyrBA*.
The pUC18 reporter plasmid was extracted from the WT and the SL1344 *gyrBA* strains at the stationary phase of growth and electrophoresed on a 0.8% agarose gel containing 2.5 µg/ml chloroquine.. The arrow shows the direction of migration, with the more supercoiled plasmid topoisomers at the right of the gel. A. Global DNA supercoiling pattern of the WT and the *gyrBA* strain when grown in LB. B. Global DNA supercoiling pattern of the WT and the *gyrBA* strain when grown in minimal medium N with high (10 mM) $MgCl_2$ or low (10 µM) $MgCl_2$. Sample lanes are supplemented with densitometry profiles that were generated with ImageJ. The analysis is representative of four biological replicates.

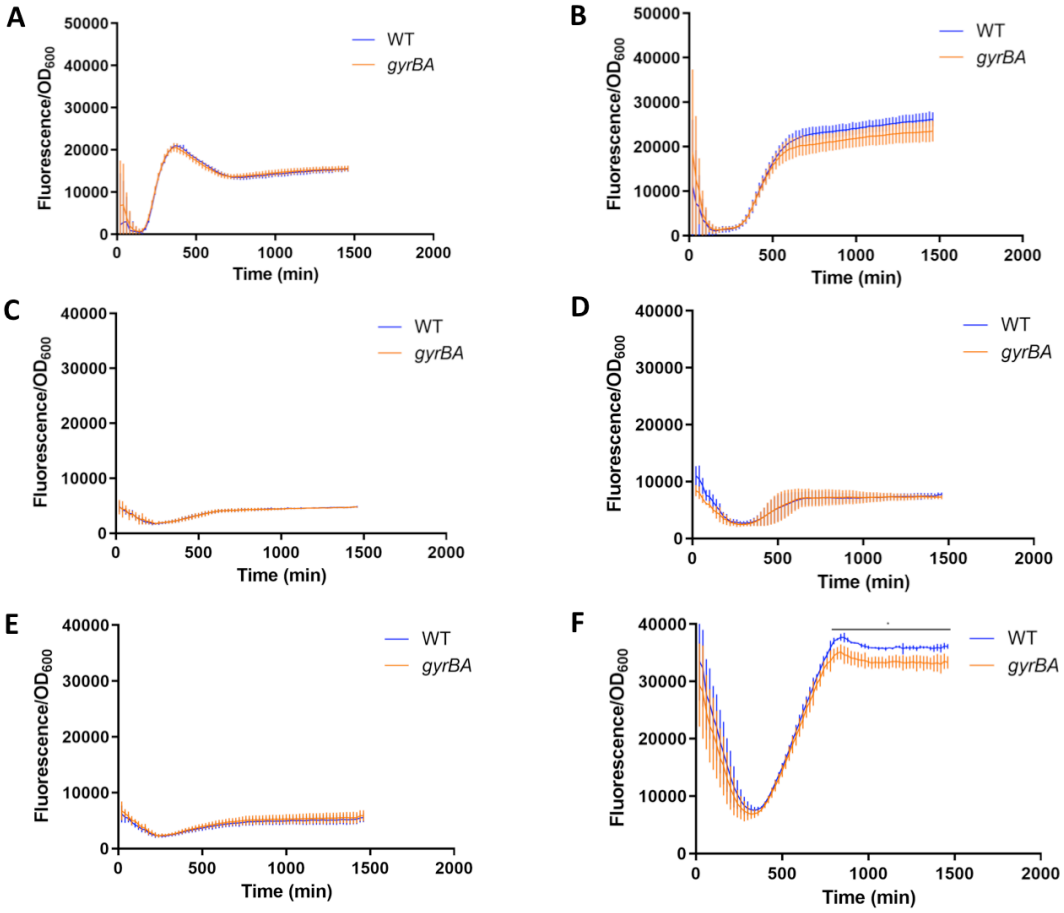

Fig. 6. Expression of genes in the SPI-1 and SPI-2 pathogenicity islands in wild type SL1344 (WT) and SL1344 *gyrBA.*

Expression of *gfp*$^{+}$ reporter gene fusions was measured in the wild type and SL1344 *gyrBA* strains every 20 min over a 24-h. period. A. SPI-1 expression in the *gyrBA* strain was identical to that in the WT in LB. B. SPI-2 expression in the *gyrBA* strain was identical to that of the WT in LB. C. SPI-1 expression in minimal medium N with high $MgCl_2$ concentration (10 mM) was repressed in both the WT and the *gyrBA* strain. D. SPI-2 expression in minimal medium N with high $MgCl_2$ concentration was repressed in both the WT and the *gyrBA* strains. E. SPI-1 expression in minimal medium N with a low $MgCl_2$ concentration (10 μM) was repressed in both the WT and the *gyrBA* strains. F. SPI-2 expression in minimal medium N with low $MgCl_2$ concentration was lower in the *gyrBA* strain than in the WT at the stationary phase of growth. All plots are the results of at least three biological replicates; error bars represent the standard deviation. Statistical significance was found by Student's unpaired T-test, where $P<0.05$.

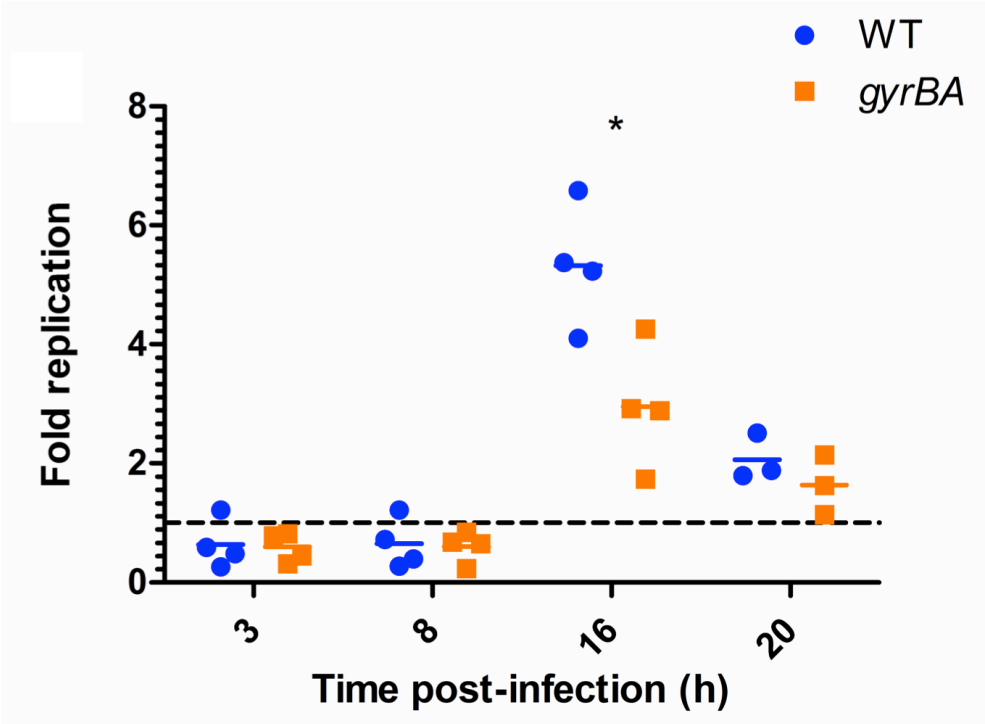

Fig. 7. SPI-1-mediated entry and survival of the WT and SL1344 *gyrBA* strain in cultured RAW264.7 macrophage cells.

Cells were infected with SPI-1-induced bacteria, grown to mid-exponential phase to promote SPI-1-mediated invasion. Survival and replication were measured by enumerating colony forming units (CFUs) at 3 h, 8 h, 16 h and 20 h post-infection. Fold replication represents the number of CFUs recovered at a particular time point divided by the CFU number at 1 h. Mean and individual replicates are shown. Significance at 16 h was found by unpaired Student's T-test, where $P<0.05$.

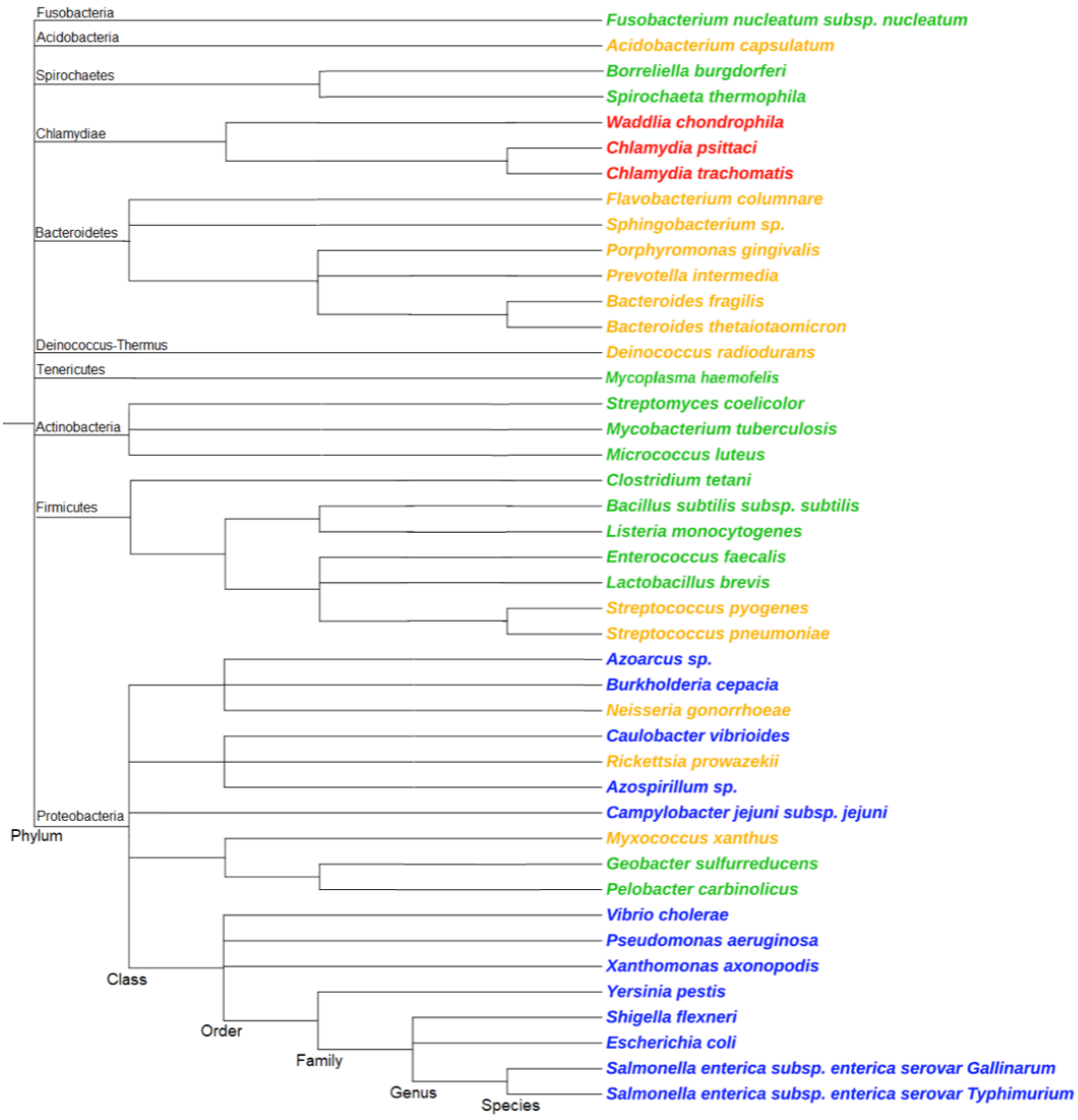

Fig. 8. Phylogenetic tree of bacteria that belong to different groups based on their *gyrA* and *gyrB* arrangement. The phylogenetic tree was built in phyloT, a phylogenetic tree generator based on NCBI taxonomy (Letunic & Bork, 2019). Each of the four groups (see Table 1) of *gyrA* and *gyrB* arrangements is indicated by colour. Group 1, blue: *gyrA* and *gyrB* are at separate locations, with a conserved genetic environment 5' to *gyrB*. Group 2, orange: *gyrA* and *gyrB* are at separate locations, with a non-conserved genetic environment 5' to *gyrB*. Group 3, green: *gyrBA* operon, conserved genetic environment 5' to *gyrB*. Group 4, red: *gyrBA* operon, non-conserved genetic environment 5' to *gyrB*. Phyla names are indicated.